UC San Diego

UC San Diego Electronic Theses and Dissertations

Title

Pharmacological inhibition of the HEG1-KRIT1 protein complex upregulate KLF2 and KLF4 expression in endothelial cells

Permalink

https://escholarship.org/uc/item/15n4k02z

Author

Choi, Chelsea Hyun Ju

Publication Date

2020

Peer reviewed|Thesis/dissertation

eScholarship.org Powered by the California Digital Library
University of California

UNIVERSITY OF CALIFORNIA SAN DIEGO

Pharmacological inhibition of the HEG1-KRIT1 protein complex upregulate KLF2 and KLF4 expression in endothelial cells

A thesis is submitted in partial satisfaction of the requirements for the degree Master of Science

in

Biology

by

Chelsea Hyun Ju Choi

Committee in charge:

Miguel A. Lopez-Ramirez, Chair
Randolph Hampton, Co-Chair
Julian Schroeder

2020

Copyright

Chelsea Hyun Ju Choi, 2020

All rights reserved.

The thesis of Chelsea Hyun Ju Choi is approved, and it is acceptable in quality and form for publication on microfilm and electronically:

_____

_____

Co-Chair

_____

Chair

University of California San Diego

2020

TABLE OF CONTENTS

LIST OF FIGURES and TABLES

ACKNOWLEDGEMENTS

I want to thank my chair, Miguel A. Lopez-Ramirez, co-chair Randolph Hampton and Julian Schroeder for serving as my committee members and guiding me through my research.

I also want to thank Dr. Lopez-Ramirez again for thesis editing and revision. I would like to acknowledge Dr. Alex Gingras, my co-mentor.

I want to recognize Preston Hale, Shady Soliman and Matthew Bautista who built foundations and helped with data collection for this thesis. I want to thank my colleagues in Ginsberg lab for their support. Lastly, I want to thank my friends and family for their endless support and love.

The part of Chapter 3 and 4 of this thesis is currently submitted for publication. The author of this thesis is also a coauthor of this pending publication. Lopez-Ramirez, Miguel; Li, Wenqing; Haynes, Mark; Hale, Preston; Choi, Chelsea; Francisco, Karol; Oukoloff Killian; Bautista, Matthew; Sun Hao; McCurdy Sara; Gongol, Brendan; Shyy, John; Ballatore Carlo; Sklar, Larry; Gingras, Alexandre .

I would also like to thank my collaborators who participated in the drug screening process; Mark K. Haynes and Larry A. Sklar from Department of Pathology, University of New Mexico School of Medicine, Albuquerque. My collaborators that performed medicinal chemistry; Killian Oukoloff , Karol Francisco and Carlo Ballatore from Department of Chemistry & Biochemistry, and Skaggs School of Pharmacy and Pharmaceutical Sciences, University of California San Diego. My collaborators that help me with gene expression analysis; Brendan Gongol and John Y. Shyy from Department of Medicine, University of California San Diego.

ABSTRACT OF THE THESIS

Pharmacological inhibition of the HEG1-KRIT1 protein complex upregulate KLF2 and KLF4 expression in endothelial cells

by

Chelsea Hyun Ju Choi

Master of Science in Biology

University of California San Diego, 2020

Miguel A. Lopez-Ramirez, Chair
Randolph Hampton, Co-Chair

HEG1 (Heart of glass1), a transmembrane protein, directly binds to and recruits KRIT1 (Krev interaction trapped protein 1) to endothelial junctions to form the HEG1-KRIT1 protein complex that establishes and maintains junctional integrity. Genetic inactivation or knockdown of endothelial HEG1 or KRIT1 leads to the upregulation of transcription factors Krüppel-like Factors 4 and 2 (KLF4 and KLF2), which are factors implicated in endothelial vascular homeostasis. However, the effect of acute inhibition of the HEG1-KRIT1 interaction remains incompletely understood. Through structure-based design, we have established the feasibility

of pharmacologically disrupting the KRIT1-HEG1 interaction to uncover acute changes in signaling pathways downstream of the HEG1-KRIT1 protein complex disruption. Previous work in the lab shows that the HEG1-KRIT1 inhibitor 3 (HKi3) is a *bona fide* interaction inhibitor by competing orthosterically with HEG1 for binding to the KRIT1 band 4.1, ezrin, radixin, and moesin (FERM) domain. In this study, we observed that acute inhibition of the HEG1-KRIT1 interaction by HKi3 triggers PI3K/Akt signaling in endothelial cells. We also observed that inhibition of KRIT1-HEG1 interaction using HKi3 also increase KLF4 and KLF2 mRNA expression levels. In addition, we developed an inducible shRNA expression system to the time-controlled knockdown of genes associated with the HEG1-KRIT1 protein complex that we denominated TRMPV-PDCD10 (tetracycline-responsive element (TRE)-dsRed-miR30-against-PDCD10-PGK-Venus). Using this RNAi system, we generated stable hCMEC/D3 cell lines, each expressing the TRMPV-*PDCD10* construct. We observed that TRMPVIR-PDCD10 doxycycline-treated cells show marked disruption of VE-cadherin staining and upregulation in KLF2 and KLF4 mRNA gene expression. Thus, our results demonstrate that acute inhibition of the HEG1-KRIT1 interaction activates PI3K/Akt activity and elevates KLF4 and KLF2 gene expression. Thus, HKi3 provides a new pharmacologic tool to study acute inhibition of the HEG1-KRIT1 protein complex. We also adopted an inducible shRNA expression system to regulate genes in endothelial cells in a time-controlled manner.

1. Introduction

1.1. Cardiovascular system

The cardiovascular system, along with the lymphatic system, is part of the body's circulation. The heart through the right ventricle pumps deoxygenated blood towards the lungs for oxygenation, and when the oxygenated blood comes back to the heart, then the left ventricle pumps the oxygenated blood to all organs through the circulatory system. The circulatory system is made of blood vessels that transport blood through the body and facilitate the exchange of oxygen, water, nutrients, and at the same time, remove waste products away from tissues (Thomas & Sumam, 2016). The blood vessels are comprised of five different segments of endothelial cells that differ in their anatomical, morphological, biochemical, and functional organization are described below in Figure 1.

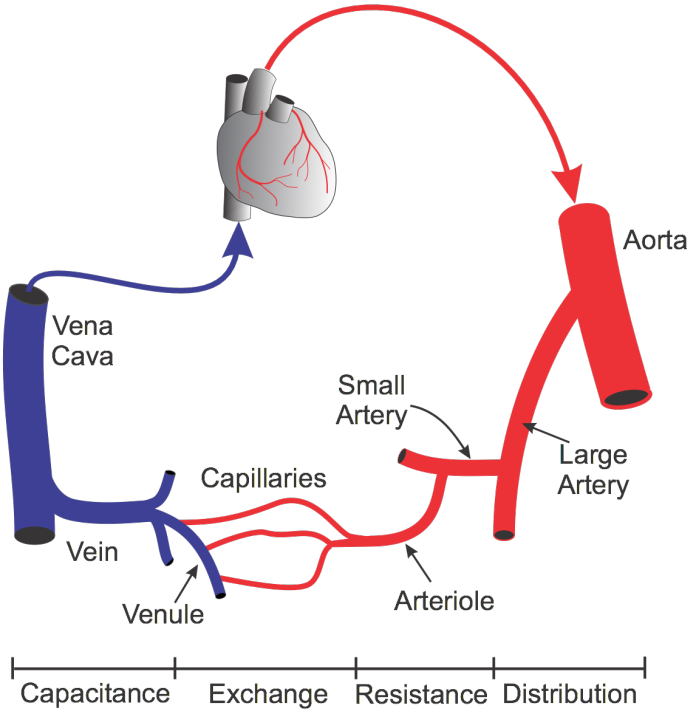

Figure 1. Different blood vessel types. From heart, blood gets transported through aorta, artery, arteriole, capillaries, venule, vein, vena cava and goes back to heart. Different types of vessels have different functions illustrated above (Klabunde, 2017)

1.1.1. Blood vessels

Arteries (4000-25000 μm diameter) carry oxygenated blood from the heart with high pressures to tissues (Müller et al., 2008). Arterioles (30 μm diameter) penetrate the tissue and play an important role in regulating flow and intravascular pressure (Müller et al., 2008). Capillaries (8 μm diameter) constitute the largest surface area for exchange between blood and tissues and facilitate the exchange of nutrients and removal of waste products (Müller et al., 2008). Venules (20 μm diameter) and veins (5000 μm diameter) carry capillary deoxygenated blood from the tissue back to the heart with low pressures (Müller et al., 2008 & Thomas & Sumam, 2016). Except for capillaries made of one layer of endothelial cells, the rest of the blood vessels have three layers. The outer layer, adventitia, provides support to vessel shape and structure. The middle layer, tunica media, is elastic and made of smooth muscular tissue to control the vessel diameter. The inner layer, tunica intima, is made of endothelial cells that directly contact with blood (Tucker & Muhjan, 2019).

1.1.2. Endothelial cells

A layer of endothelial cells (EC) in blood vessels is called the endothelium. Basal lamina, connective tissues, and smooth muscle surround endothelium. The basal lamina or endothelial basement membrane separates the endothelium from the connective tissues and smooth muscle cells (Alberts et al., 2002). In capillaries, blood vessels consist of endothelial cells and pericytes, which are surrounded by a basal lamina. Importantly, endothelial cells sense the shear stress from blood flow and regulate blood vessel diameter and thickness (Alberts et al., 2002). Brain endothelial cells compose the main parts of the blood-brain barrier (BBB). BBB ECs regulate ion

homeostasis in CNS by their selective permeability and protect CNS from toxin and pathogen entry (Daneman & Prat, 2015).

1.1.3. Pericytes

Pericytes are mural cells that wrap the surface of the abluminal side of the endothelium in capillaries to give structural support. It is known to be abundant in blood vessels at torso and legs, the site where more blood pressure is needed (Bergers & Song, 2005). Pericytes interact with EC through paracrine signaling and through physical contact via gap junctions (Bergers & Song, 2005). Gap junction between pericyte and EC allows the exchange of small molecules such as amino acids, secondary messengers and ions (Okamoto et al., 2017 & Bergers & Song, 2005).

Pericyte density and coverage location are often specific to organ or tissue functions. For instance, the brain vasculature is highly populated by pericytes, where they interact with brain endothelial cells to induce and regulate the BBB (Bergers & Song, 2005). Pericytes have also being recognized to regulate capillary blood flow by virtue of their contractile properties and to have macrophage-like phagocytic function. The loss of brain pericytes leads to BBB dysfunction and contributes to brain diseases (Bergers & Song, 2005). Similarly, the loss of cardiac pericyte leads to the accumulation of myocardial interstitial fluid and contributes to heart dysfunction (Murray et al., 2017).

1.1.4. Smooth muscle cells

In contrast to small blood vessels, large vessels tend to have many layers of smooth muscle cells. For example, smooth muscle cells sporadically cover veins, but many layers of

smooth muscle cells support arteries for high blood pressure. Moreover, smooth-muscle cells play an important role in regulating blood flow through contractile functions and maintaining structural support (Bergers & Song, 2005). These cells are present in the middle layer of a vessel, tunica media. Although smooth muscle cells are quiescent normally, they can remodel their phenotype, gene expression, and function during injury and disease (Mazurek et al., 2017).

1.1.5. Basal lamina

The basal lamina separates connective tissues and endothelium in blood vessels. The basal lamina is a type of extracellular matrix (ECM) composed of elastic lamellae, collagen fibers, microfibrils, fibronectin, proteoglycans, and glycoproteins (Mazurek et al., 2017). The major components are elastic lamellae and collagen fibers that provide elastic and tensile strength to vessels (Mazurek et al., 2017). ECM provides support to endothelial cells from the maintenance of cell organization to blood vessels. Endothelial cells need to adhere to ECM for cell proliferation, survival, migration, morphogenesis, and stabilization (Davis & Senger, 2005).

1.2. The function of the endothelial cells

The functions of endothelial cells, in addition to transport blood, nutrients and oxygen include the maintenance of vascular tone and also exhibit anticoagulant and anti-inflammatory properties that limit thrombosis to maintain vascular homeostasis (Michiels, 200). These anti-inflammatory and thrombo-resistant properties of endothelial cells are enhanced by laminar blood flow that regulates multiple molecular processes including the synthesis of vasoactive, anti-inflammatory, and anti-thrombotic molecules (Chiu & Chien, 2011). The loss of these endothelial functions is associated with increased cardiovascular morbidity (Versari et al., 2009

& Chiu & Chien, 2011). In addition, endothelial cells provide barrier properties to regulate the exchange of protein, fluid, and electrolyte between tissue and blood (Shen et al., 2009).

1.2.1. Coagulation

ECs initiate and regulate coagulation cascade (Wang et al., 2018). EC secretes substances that regulate coagulation and platelet adhesion to endothelium, including thrombomodulin (TM) and Von Willebrand factor (VWF) (Wang et al., 2018). For instance, during hemostasis, which is the physiological process to prevent and stop bleeding (Arrieta-Blanco et al., 2014), platelets get activated by interaction with endothelial cells after being exposed to the extracellular matrix (ECM) from disrupted endothelium (Wang et al., 2018). After platelet activation, coagulation factor VII binds to tissue factor or factor XII, and the rest of the coagulation cascade continues to prevent bleeding (Wang et al., 2018). Fibrin is another important component in clot formation. As a matrix in a blood clot, fibrin stabilizes platelet aggregation at the site of injury for the long-term (Michiels, 2003 & Palta et al., 2014). Fibrin is activated by Thrombin protease, which is activated by Factor Xa (Michiels, 2003). Importantly, the endothelium expresses natural anticoagulant proteins, including thrombomodulin (TM) and endothelial protein C receptor (EPCR) (Michiels, 2003). TM binds thrombin, while bound, thrombin fails to convert fibrinogen into insoluble fibrin, and instead, it activates protein C. Activated Protein C, which is enhanced by the presence of EPCR, inactivates factor Va and VIIIa to prevent blood coagulation. (Michiels, 2003). Therefore, EC exhibits anti-coagulation activity through activated protein C to maintain blood flow and vascular homeostasis. However, during cardiovascular disease and chronic inflammation, EC can shift toward a pro-coagulation state by reducing the expression of anti-coagulant proteins that can result in thrombosis (a pathological occlusion of blood vessels)

(Michiels, 2003). Moreover, during blood vessel injury vWF in endothelial cells induce thrombosis formation by promoting platelet adhesion and inflammation (Wang et al., 2008).

1.2.2. Inflammation

Many cardiovascular diseases, such as atherosclerosis and thrombosis contain an important inflammatory component that contributes to endothelial dysfunction (Szmitko et al., 2003). Immune cells produce pro-inflammatory cytokines that lead to increased endothelial permeability, which is associated with changes in EC phenotype and function (Pober & Sessa, 2007). For instance, during inflammation, EC increases the expression of ICAM-1 (Intercellular Adhesion Molecule 1), VCAM-1 (Vascular Cell Adhesion Molecule 1), and selectins to attract and adhere leukocytes to the endothelium that subsequently contribute to increasing paracellular permeability (Parnell et al., 2012). The molecular mechanism identified to increase permeability are associated with actomyosin contraction which leads to transient paracellular opening (Shen et al., 2009), apoptosis that leads to gross changes in permeability (Gill et al., 2015), and dissociation of junctional complex molecules from cell-to-cell contacts (Reglero-Real et al., 2016).

1.3. Barrier properties

EC serves as semipermeable barriers in the body. The primary function of the barrier is to facilitate nutrient and waste exchange and to limit the entry of pathogens or any toxins (Yuan & Rigor, 2010). Endothelial barriers have different permeability due to the complexity of endothelial junctions.

1.3.1. Endothelial junctional molecules

The junctional complex in EC is comprised of adherens junctions, tight junctions, and gap junctions (Komarova et al., 2017). In Adherens junctions, vascular endothelial (VE)-cadherin, a transmembrane protein, mediates cell-to-cell contact between endothelial cells. VE-cadherin also supports barrier properties by regulating tight junction expression in EC (Komarova et al., 2017). Tight junctions form the border between the apical and the basolateral cell surface domains that seal the intercellular space (Förster, 2008). Tight junctions are located at the border between the apical and the basolateral cell surface domains and seal the intercellular space (Komarova et al., 2017). Gap junctions have channels consisted of connexin molecules that connect between endothelial cells for the conduction of ions (Komarova et al., 2017).

1.3.2. Adherens junctions

VE-cadherin stabilizes endothelial cell interaction by forming zipper-like structures. Endothelial junctions have unique features that differentiate from other cell junctions. VE-cadherin (CDH5/CD144) is only expressed in endothelial cells and is a major cadherin type at adherens junctions (Bazzoni & Dejana, 2004). VE-cadherin is anchored to actin through binding

with intracellular β-catenin through cytoplasmic tails. This actin-adherens junction is critical for adherens junction maintenance and assembly (Dejana & Orsenigo, 2013). β-catenin and VE-cadherin complex may also affect transcription by translocation into the nucleus (Bazzoni & Dejana, 2004). Another type of Cadherin, N-cadherin, facilitates the communication between EC and surrounding pericyte/smooth muscle cells to stabilize blood vessels (Komarova et al., 2017).

1.3.3. Tight junctions

Tight junctions consist of three different types of transmembrane proteins, such as claudin family (1 to 12), occludin, and junctional adhesion molecules (JAM). Endothelial tight junctions indirectly interact with the actin cytoskeleton through adaptor and scaffolding proteins, such as members of the zonula occludes (1 to 3). (Komarova et al., 2017). ZO-1 helps tight junction molecules to interact with other ones and interact with Adherens Junction to control the barrier permeability (Sukriti et al., 2014). Transmembrane protein, Claudin 5 is important in controlling permeability of tight junction, especially in the BBB. Occludin, integral membrane protein, acts to stabilize the barrier functions by promoting cell to cell adhesion (Bazzoni & Dejana, 2004). Tight junctions are more abundant in the arterial side of circulation than the venular side. JAM-A, B, and C are involved in leukocyte migration in between endothelial cells. JAM-A may play a critical role in transmigration of neutrophils in between EC. Adherens junctions can also regulate tight junctions. For example, VE-cadherin leads to the upregulation of claudin 5 that only appears at tight junctions (Taddei et al., 2008). Brain endothelial cells have complex tight junctions that prevent paracellular transport (transport across endothelial cells through intercellular space) (Katt et al., 2016). Disruption of adherence and tight junctions have

been associated with loss of barrier integrity that contributes to CNS disease during neuroinflammation (Komarova et al., 2017).

1.4. Mechanism that establish and maintain junctional integrity

As mentioned above, endothelial junctional integrity is maintained by VE-cadherin. In endothelial cells, high levels of cAMP (cyclic adenosine monophosphate) activate Rap1 (Ras-related protein1) to maintain mature endothelial junctions. Rap1 plays an important role in the maintenance of both adherens junctions and tight junctions. Rap 1 is necessary for VE-cadherin mediated cell adhesion. Although the exact mechanism is unknown, Rap1 decreases cell permeability by enhancing VE-cadherin mediated cell-adhesion (Fukuhara et al., 2005). Rap1 mediates the cell-adhesion property of VE-cadherin with β-catenin. In tight junctions, the absence of Rap1 activity is immediately followed by the loss of ZO-1 proteins, which controls tight junction permeability (Kooistra et al., 2006 & Sukriti et al., 2014). The loss of Rap1 activity eventually leads to the loss of tight junctions (Kooistra et al., 2006).

1.4.1. Heart of glass 1 (HEG1)

HEG1(Heart of glass 1) is a transmembrane protein with 400 kDa. HEG1 plays an important role in cardiovascular system development and regulation of heart growth in mouse and zebrafish (Kleaveland et al., 2009) (Tsuji et al., 2017). HEG1 is expressed in endothelial cells at the embryonic developmental stage (Kleaveland et al., 2009), where it interacts with KRIT1 (Krev interaction trapped protein 1) (Gingras et al., 2013) to regulate endothelial junctions (De Kreuk et al., 2015).

1.4.2. Krev interaction trapped protein 1 (KRIT1)

KRIT1 can be divided in several domains including; C-terminus FERM domain (4.1, ezrin, radixin, moesin), N-terminus NPX(Y/F) motifs and ankyrin repeats (Gingras et al., 2013). KRIT1 is located at autosomal dominant loci, 7q21 (Gunel et al., 2002). NPX(Y/F) motifs interact with CCM2 (Fisher et al., 2014). Ankyrin repeats, made of 4 repeats, interact with C-terminal FERM domain and form a globular Ankyrin repeat-FERM domain (Zhang et al., 2015). KRIT1 size is about 62 kDa (Gunel et al., 2002).

KRIT1 stabilizes Rap1 at endothelial junctions and maintains junctional integrity. Moreover, KRIT1 interacts with β-catenin to link the actin cytoskeleton to VE-cadherin that strengthens adherens junctions. KRIT1 is part of the cerebral cavernous malformation (CCM) protein complex which, consists of four proteins: CCM1 (KRIT 1), CCM 2, CCM 3 (PDCD 10, Programmed Cell Death 10), and HEG1. Disruption of any CCM proteins leads to an increase in vascular permeability by disassembling of endothelial junctions (Dejana & Orsenigo, 2013).

1.4.3. HEG1-KRIT1 interaction

The transmembrane protein HEG1 binds directly to and recruits KRIT1 to EC cell junctions to regulate and maintain the organization of junctional molecules, which are critical for vertebrate cardiovascular development (Kleaveland et al., 2009, & Gingras et al., 2012 & Gingras et al., 2013 & Glading & Ginsberg, 2010). Our group has solved the crystal structure of the HEG1-KRIT1 protein complex (Gingras et al., 2013 & Gingras et al., 2012) and found that the KRIT1 FERM domain binds to the HEG1 cytoplasmic tail C-terminus. These experiments revealed a new mode of FERM domain-membrane protein interaction. The KRIT1 FERM domain consists of three subdomains (F1, F2, and F3) forming a cloverleaf shape in which the F1

and F3 subdomain interface creates a hydrophobic groove that binds the $Tyr^{1,380}$-$Phe^{1,381}$ of the most C-terminal portion of the HEG1 cytoplasmic tail (Gingras et al., 2012). Moreover, the KRIT1 FERM domain also simultaneously binds to another protein named Rap1, a small GTPase, on the surface of the F1 and F2 subdomains to stabilize endothelial junctions by forming the HEG1-KRIT1-Rap1 ternary complex (Gingras et al., 2013 & Glading & Ginsberg, 2010 & Li et al., 2012). These studies suggest that part of the biological effects of KRIT1, related to endothelial junctional integrity, relies on the KRIT1 FERM domain being recruited to cell-cell junctions to interact with both HEG1 and Rap1.

HEG1 and KRIT1 are also genetically linked in mice (Kleaveland et al., 2009) and zebrafish during cardiovascular development (Kleaveland et al., 2009 & Donat et al., 2018 & Mably et al., 2003). *Krit1*$^{-/-}$ mice show gross defects in multiple vascular beds and early embryonic lethality (Whitehead et al., 2004). Similarly, *Heg1*$^{-/-}$ mice result in lethal hemorrhage due to cardiovascular defects (Kleaveland et al., 2009). Studies in zebrafish embryos show that loss-of-function *of krit1* or *heg1* leads to vascular dilation and severe heart defects (Kleaveland et al., 2009 & Hogan et al., 2008 & Mably et al., 2006). It has been demonstrated that increases in endothelial KLF4 and KLF2 may constitute a major mechanism by which loss of HEG1 or KRIT1 alters cardiovascular development (Cuttano et al., 2015 & Bharadwaj et al., 2010 & Zhou et al., 2016 & Lopez-Ramirez et al., 2017 & Nowak et al., 2010)

1.5. Mechanism that maintain endothelial integrity

Vascular endothelial cells respond to hemodynamic forces from blood flow to exhibit vasodilatory, anticoagulant, fibrinolytic, and anti-inflammatory properties that confer vasoprotective effects that play a critical role in maintaining healthy vasculature (Baeyens et al., 2016). Many of the vasoprotective effects of laminar blood flow are due to upregulation of

transcription factors Kruppel-like factors 2 and 4 (KLF2 and KLF4), which in turn can increase expression of genes that encode anticoagulants (e.g., TM), vasodilators (e.g., endothelial nitric oxide, eNOS), and suppress the expression of genes that antagonize angiogenesis (e.g., thrombospondin1, TSP1) and NF-kB-driven proinflammatory genes (e.g., VCAM1 and ICAM1) (Abe & Berk, 2014 & Kim et al., 2017 & Peghaire et al., 2019). Thus, laminar flow can upregulate KLF2 and KLF4 in endothelium to antagonize inflammation, and thrombosis (Nayak et al., 2011). However, subtle deficiencies in endothelial cell function or response to blood flow greatly affect vascular physiology and contribute to onset and progression of cardiovascular diseases (Biswas & A. Khan, 2019).

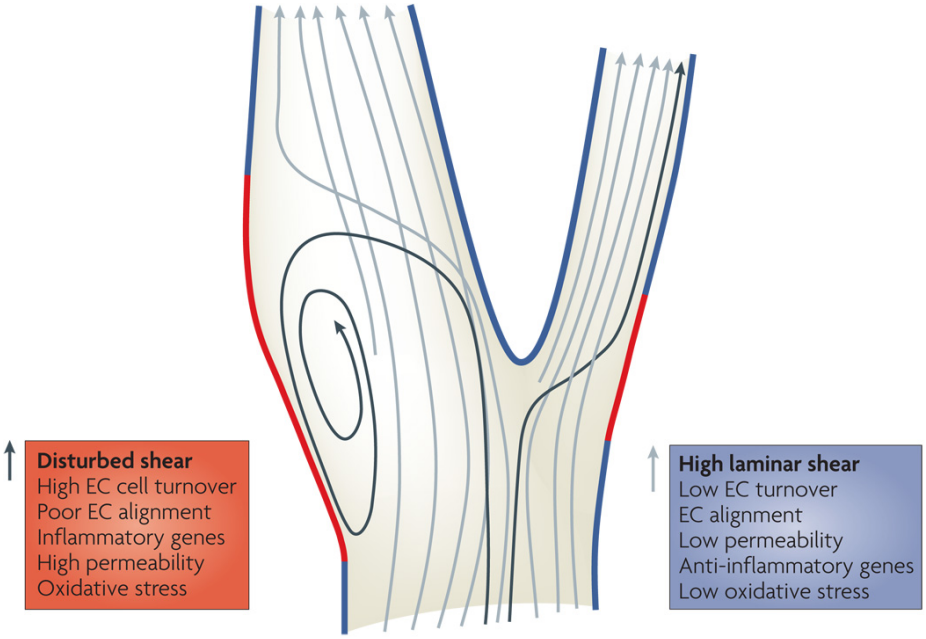

Figure 2. Shear stress exerted to a blood vessel following laminar and non-laminar flow. At the site of bifurcation of arteries (red), non-laminar flow pattern and disturbed shear stress are observed. These regions have lower flow and have inflammatory gene upregulated (Hahn & Schwartz, 2009).

1.5.1. Laminar blood flow

Laminar blood flow (laminar shear) has a flow direction parallel to blood vessels (Chatterjee & Fisher, 2014). In a blood vessel, fluid shear stress (the frictional force that blood flow exerts on endothelial cells) is exerted in the same direction as laminar blood flow (Hahn & Schwartz, 2009), so that both adherens and tight cell junction assembly is promoted and increase intercellular force (Ting, 2012). Different fluid velocity in laminar flow leads to fluid shear stress sensed on the vascular wall. Friction between fluid and vascular wall decreases blood velocity nearest to the vessel. Poiseuille's law, Q (flow) = P /R states that blood flow is inversely proportional to vessel resistance and directly proportional to pressure (Pollock et al., 2020). If vascular resistance is high, blood flow is low and vice versa. If more force is generated by the heart to pump blood, blood flow is high (Pollock et al., 2020). Importantly, non-laminar flow (disturbed shear) is present at branch points and curves of vessels where the blood flow is irregular in Figure 2. (Hahn & Schwartz, 2009). Disturbed shear can lead to pathological vascular remodeling, especially atherosclerosis and thrombosis (Thomas & Sumam, 2016 & Baeyens et al., 2016). Moreover, it has been reported that disturbed shear contributes to inflammation by increase in expression of VCAM and ICAM (Chiu & Chien, 2013) and disassembly of tight and adherns junctions in endothelial cells contributing to endothelial barrier breakdown (Ting, 2012 & Hahn & Schwartz, 2009).

1.5.2. Mechanotransduction complex

Endothelial cells have many mechanosensors to sense shear stress (Alberts et al., 2002). Mechanosensors include integrins, cytoskeletal proteins, endothelial cell adhesion molecule 1, and ion channels. Shear stress triggers a cascade of intracellular cell signaling and regulates

shape, vessel tone, inflammation, and apoptosis by altering gene expression of KLF and eNOS (Figure 3) (Noguchi & Jo, 2011). Previous studies have shown that mechanotransduction via fluid shear stress mediates MEK5 /ERK5 (Mitogen-activated protein kinase kinase 5-extracellular regulated kinase 5) and PI3K/Akt (phosphatidylinositol 3-kinase-Protein Kinase B) activation (CLARK et al., 2011 & Coon et al., 2015 & Jin et al., 2003 & Jin et al., 2005). Shear stress from laminar blood flow initially activates MAP kinase kinase, MEK5, MEK5 then phosphorylates ERK5 and leads to upregulation of transcription factor MEF2A, C and D. These transcription factors upregulate KLF2 and KLF4 (CLARK et al., 2011).

Mechanistically, fluid shear stress increases tension on PECAM1 and subsequent activation of Src family kinases-induced ligand-independent VEGFR2/3 activation that, in turn, activates PI3K (Coon et al., 2015 & Jin et al., 2003 & Baeyens et al., 2016). In addition, Rap1 has been proposed to be activated by laminar shear stress to promote the endothelial mechanosensing protein complex by increasing the association between PECAM1-VEGFR2/3-VE-cadherin and subsequent PI3K/Akt signaling (Lakshmikanthan et al., 2015). Increase in Akt signaling mediates phosphorylation of eNOS (endothelial nitric oxide synthase) and leads to the release of nitric oxide for vasodilation (Lee, 2014 & Lakshmikanthan et al., 2015) and mitogen-activated protein kinases (MAPK) signaling pathways involved in many other cellular processes such as cell survival (Ruan & Kazlauskas, 2012), anti-inflammatory pathways and anti-apoptosis pathways (Noguchi & Jo, 2011).

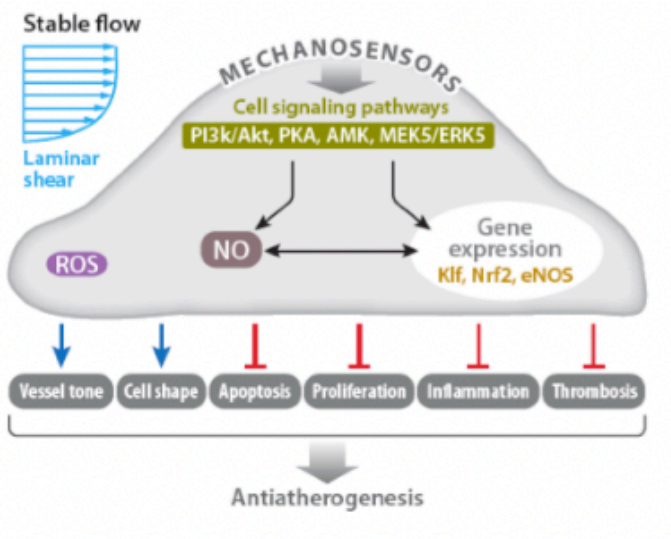

Figure 3. Laminar flow induced mechanotransduction in endothelial cells. Stable laminar flow activates cell surface mechanosensors and triggers cell signaling cascade that alternates gene expression. Mechanotransduction leads to antiatherogenic process (Noguchi & Jo, 2011).

1.5.3. Expression of Krüppel-like factor 2 (KLF2) and Krüppel-like factor 4 (KLF4) in endothelial cells

MAPKs are conserved serine/threonine kinases involved in flow-induced mechanotransduction through upregulation of Krüppel-like factor 2 and 4 (KLF2 and KLF4) expression.

As mentioned in 1.5.2, MEK5 is a MAP kinase that is upstream of ERK5, which is also a MAP kinase. ERK5 translocates into the nucleus and activates transcription factor MEF2 family (MEF2A, c, d) (Gomez et al., 2016). MEK5-ERK5-MEF2 mechanotransduction module regulates KLF4 and KLF2 expression during laminar blood flow (Chistiakov et al., 2016 & Gore et al., 2012) to confer vascular integrity (Huddleson et al., 2005) and vasoprotection (Parmar et al., 2005).

Recently our group and others demonstrated that genetic inactivation or knockdown of endothelial HEG1 or KRIT1 leads to the increase of transcription factors KLF2 and KLF4

(Nowak et al., 2010 & Lopez-Ramirez et al., 2017 & Bharadwaj et al., 2010 & Cuttano et al., 2015 & Zhou et al., 2016). Using RNA-sequencing analysis of murine endothelial cells following time-controlled inactivation of the *Krit1* gene revealed increased levels of several vasoprotective genes regulated by KLF2 and KLF4, including eNOS and TSP1 (Lopez-Ramirez et al., 2017) and anticoagulant protein TM (Lopez-Ramirez et al., 2019). These findings lead us to propose that pharmacological inhibition of the KRIT1-HEG1 protein complex can be used to upregulate KLF2 and KLF4 and may, therefore, be able to mimic laminar blood flow to attenuate inflammation, thrombosis and atherosclerosis.

1.6. Hki3 as an effective inhibitor of HEG1-KRIT1 interaction in endothelial cells

My co-supervisor Dr. Alex Gingras performed a high-throughput screening assay and molecular design of a small molecule HEG1-KRIT1 inhibitor to study acute changes in signaling downstream of the HEG1-KRIT1 protein complex disruption not previously studied (Lopez-Ramirez et al., 2019). Using crystal structure analysis, Dr. Gingras demonstrated that the HEG1-KRIT1 inhibitor 3 (HKi 3) binds to the KRIT1 FERM domain in the same site as it will normally interact with HEG1 cytoplasmic tail (Figure 4). His studies reveal that HKi3 is a bona fide inhibitor by competing orthosterically with HEG1 for binding to the KRIT1 FERM domain.

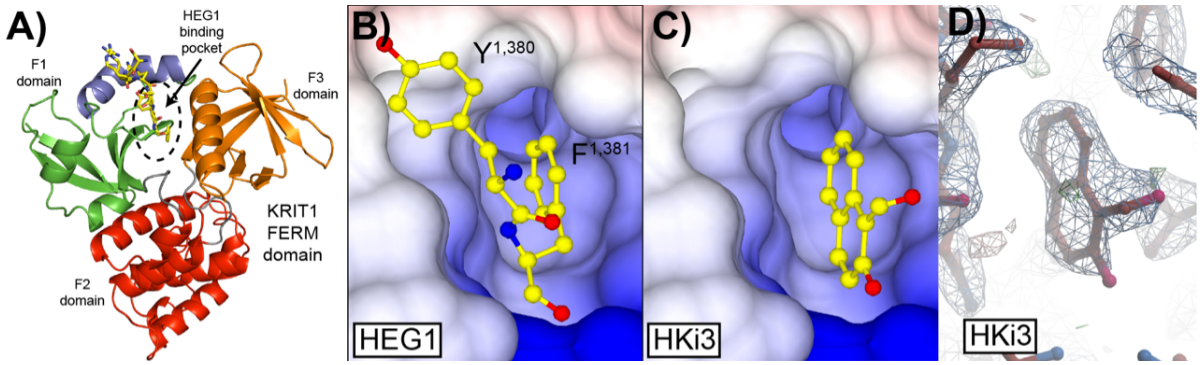

Figure 4. Structure of KRIT1 with inhibitor HKi3. (A) Ribbon diagram of the KRIT1 FERM domain in complex with the HEG1 cytoplasmic tail. The KRIT1 FERM domain consists of three subdomains. (B) Surface representation of KRIT1 FERM domain in complex with the HEG1 cytoplasmic tail. The HEG1 peptide is shown in yellow with the C-terminal Tyr-Phe sitting in the binding pocket. (C) Crystal structure of the KRIT1 FERM domain in complex with HKi3 (2-hydroxy-1-naphthaldehyde). The small naphthalene is sitting in the same pocket as the Phe of HEG1 and (D) good electron density is observed.

1.7. Objectives of the present study

Cardiovascular diseases are currently the main cause of death in the world and morbidity is usually due to thrombosis and inflammation. We have discovered that genetic inactivation of endothelial *Krit1* (Krev1 interaction trapped gene1, also known as CCM1) or *Heg1* (Heart of glas1) mimic changes in gene expression to be induced by flow-mediated vasoprotection such as upregulation of KLF4 and KLF2. Given the discovery of a small-molecule HKi3 a pharmacological inhibitor of the HEG1-KRIT1 protein complex, we aimed to assess the potential use of this small molecule as a potential vasoprotective strategy and as a new tool to identify the downstream signaling pathways of the HEG1-KRIT1 protein complex.

Hence, the aims of the present work are:

1.- To evaluate the effects of HKi3 on acute changes in signaling downstream of the HEG1-KRIT1 protein complex disruption.

2.-To evaluate the effects of HKi3 on endothelial mRNA KLF2 and KLF4 expression levels.

3.-To establish a human brain endothelial cell-line, hCMEC/D3, that contain a time-controlled inactivation of *KRIT1* or *HEG1* gene expression.

2. Materials and Methods

2.1. Growth surface preparation for endothelial cells

For HUVEC, the surface was coated with 1 % gelatin in Phosphate-buffered saline (PBS). For hCMEC/D3 cells, the surface was coated with collagen type I (C8919, 0.1 % (w/v) in 0.1 M acetic acid) stock diluted 1 in 20 in Hank's balanced salts solution with calcium (142502, Sigma-Aldrich) and incubated at 37 °C for 1 hour.

2.2. Cell media preparation

For HUVEC and hCMEC/D3 cells, 0.025% recombinant human EGF, 0.1% insulin-like growth factor, 0.1% gentamycin, 0.04% ascorbic acid, 0.04% hydrocortisone, and 20% FBS (Fetal Bovine Serum) were defrosted in 37 °C water bath then added to EGM™-2 Endothelial Cell Growth Medium-2 (LONZA). For 293 cell media, FBS, Penicillin, streptomycin and non-essential amino acids were added to DMEM media.

2.3. Cell culture

The cells frozen in 10% DMSO were defrosted in 37 °C water bath and then washed with 13 mL of 293 media and centrifuged at 5000 rpm for 5 minutes. The cells were resuspended in EGM-2 media (Methods 2.2). After reaching confluence, cells were washed with HBSS without calcium (142502, Sigma-aldrich) twice. Trypsin 0.05% (HUVEC, 293 cells) or 0.25 % (D3 cells) were added and incubated for 3-5 minutes. Trypsinzed cells were washed with 293 media and centrifuged at 5000 rpm for 5 minutes. The cell pellets were resuspended in EGM-2 media (Method 2.2) and grown to confluence at 37 °C in 95% air and 5% CO_2.

2.4. RNA isolation

The cells were lysed with 1000 µl of Trizole (Thermofischer Sceintific) and stored in –80 °C. The cell lysate in Trizol and glycoblue were defrosted on ice. The cell lysate was

transferred to a yellow phase-separation tube (2302830; VWR) and 200 µl of isopropanol (ICN19400290; Thermo Fischer Scientific) was added to cell lysate. The cell lysates were centrifuged at 4 °C at 12000 g for 10 minutes. The clear top phase was transferred to the new RNase free tube. The blue precipitate was left to dry until the precipitate became a gel-like state. The blue precipitate was resuspended in 13 µl of RNase free water. The RNA sample was quantified with NanoDrop1000 Spectrophotometer. Based on the concentration determined at 2.4.

2.5. RT-qPCR

For cDNA synthesis, 1µl of RNA (10ng/ul) was mixed with a master mix with 2 µl of random primers at 10 µM. The mixture was placed in a thermal cycler at 25°C for 10 minutes (C1000 Touch, Bio-Rad). The second master mix was added after 10 minutes and the reaction was carried out for 1 hour at 50°C (48190011; 18080093; Thermo Fischer Scientific). Then the reaction was placed at 70°C for 15 minutes. 10 µl of DNAse/RNAse free water was added to cDNA. For RT-qPCR, 1 µl of cDNA was added to 2 µl of human primers: β-actin, KLF2, KLF4, CCM3/PDCD10, HEG1, eNOS. The samples were all run in duplicates. Kapa SybrFast qPCR mix was added to primers and cDNA (Kapa Biosystems). RT-qPCR was carried out with a thermal cycler21 (C1000 Touch, Bio-Rad). The cycle steps were listed: 95°C for 15 minutes, 40 cycles with 30 seconds at 95°C, 30 seconds at 55°C, and 30 seconds at 72°C. Based on the quantification data, Threshold cycle values were calculated.

dCT = mean values of sample – mean value of Actin

ddCT = mean value of with tetracycline – mean value of without tetracycline

mRNA expression level = 2 power – ddCT (fold-difference)

2.6. Western Blot

The cells were first washed with cold HBSS with Calcium buffer (142502, Sigma-aldrich) twice and lysed with 300 µl of cold RAPI buffer (4 mL RAPI buffer and 1 tablet of protease inhibitor). The samples were frozen at -80 °C. The frozen sample were defrosted on a rotator for 1 hour at 4 °C. A BCA assay was performed to quantify the cell lysate (500-0116, Thermo Scientific). 2X Laemmli sample buffer were added to each lysate with 30 µg of protein and heated at 90 °C for five minutes. The samples were loaded into 4% to 20% sodium dodecyl sulfate-polyacrylamide gel (XP04200, Thermo Fischer Scientific) and 0.4 % SDS-PAGE gel well. The voltage was 40 V for 1 hour. Nitrocellulose membrane (Amersham) and the gel were stacked in a cassette and placed in a chamber filled with 4 °C transfer buffer. The transfer was done at 4 °C for 16 hours at 30 V. The membrane was stained with ponceau solution for five minutes, washed with PBS for three times and blocked at 10 % milk at PBS. The membrane was placed in a wet chamber in suspension of 1:100 primary antibody dilution in 1xTris-buffered saline (TBS) at 4 °C overnight. The membrane was washed with PBS three times. Then 1:1000 secondary antibody dilution in PBS was added to the membrane for 1 hour at room temperature on a shaker. After secondary antibody, the membrane was washed with PBS three times.

Lysis solution: radioimmunoprecipitation assay (RIPA) buffer [25mM Tris/HCl pH 7.6, 1% NP-40, 150mM NaCl, 1% sodium deoxycholate, 0.1% sodium dodecyl sulfate (SDS)], 1mM sodium orthovanadate, protease inhibitor (11836170001, Roche)

Laemmli's sample buffer (4x):, 40% glycerol, 8% SDS, 15mg/ml D,L-dithiothreitol, 0.01% bromophenol blue in 250mM Tris/HCl (pH 6.8)

Running buffer: 1M glycine, 125mM Trizma base and 0.01% (v/v) SDS in ddH2O.

Transfer buffer: 50mM Trizma base, 40mM, 20% (v/v) methanol in ddH2O

Blocking buffer: 0.1% tween-20, 10% fat-free dried milk dissolved in TBS at pH 7.4.

Washing buffer: 0.1% tween-20 dissolved in TBS at pH 7.4.

Molecular weight marker: Precision Plus Protein dual color standard (1610374, BioRad).

2.7. Immunohistochemistry

The cells placed on coverslip (Method 2.14) were washed with warm Hank's balanced salts solution with calcium (142502, Sigma-Aldrich) two times and fixed in 4% PFA for 10 minutes. The coverslips were blocked for 10 minutes and permeabilized for an hour (0.5% Triton X-100, in PBS). The cells were washed three times in PBS shaking at room temperature. The primary rabbit antibodies against VE-cadherin (1:300, Cell signaling) were incubated at room temperature with overnight. The cells were washed three times in PBS and incubated with Goat anti-rabbit secondary antibodies conjugated to Alexa Fluor 488 (1:300, Life Sciences) at room temperature for 1 hour.

2.8. Tetracycline-inducible vector construct synthesis

The TRMPV (TRE-dsRed-miR30-against-PGK-Venus) vector was obtained from Addgene and directed to specific genes following previous report (Zuber et al., 2019).

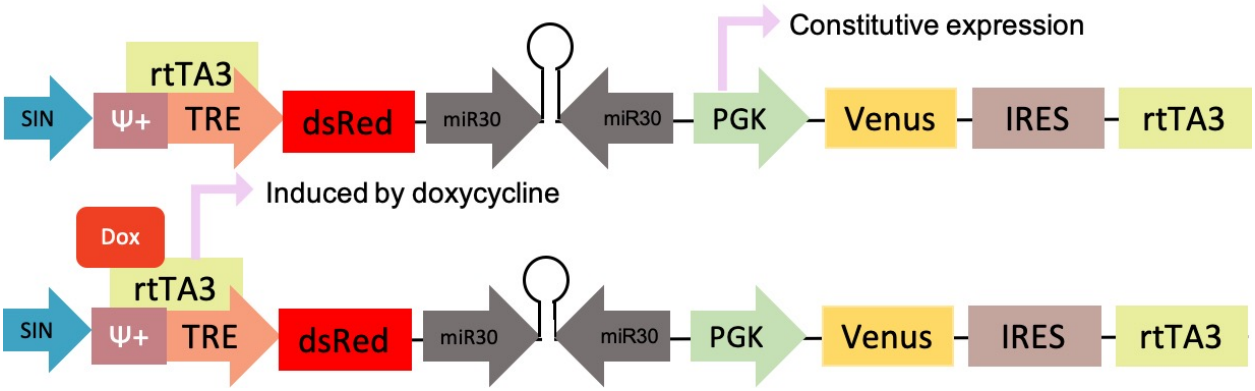

Figure 5. TRMPIVR vector construct. The top shows constitutive expression of vector when tetracycline is not present. PGK promoter is active and transcribes Venus. The bottom shows the vector when doxycycline is present. Doxycycline drives the TRE promoter expression and transcribes dsRED and downstream miR with shRNA insert.

2.9. Vector Insert preparation

shRNA oligomer sequences specific for CCM3(PDCD10), HEG1, CCM1(KRIT1) target were designed and amplified via PCR. The amplified oligomers were confirmed with gel electrophoresis and purified following the manufacturer's protocol (Qiagen Endotoxin-free Maxiprep). The oligomers were inoculated at 2-5 mL of LB broth with penicillin. The broth was incubated for 12 hours at 37°C with shaking at 300 rpm. The starting culture was diluted in 100 mL of medium. The diluted culture was grown at 37°C for 16 hours with shaking at 300 rpm. The cells were collected by centrifuging at 4 °C for 15 minutes at 6000 g. The pellet was resuspended with 4 mL of buffer P1 with RNase A addition. The pellet was thoroughly resuspended with vortex. Buffer P2 10 ml was added and inverted 4 to 6 times. The mixture was incubated at room temperature for 5 minutes for the viscous lysate. 10 mL of Buffer P3 kept at 4 C was added and inverted 4 to 6 times and incubated on ice for 20 minutes and centrifuged at 4°C at 20,000 g for 30 minutes. The supernatant with DNA was separated and centrifuged again at 20,000 g at 4 °C for 15 minutes. QIAGEN-tip 500 was equilibrated with 10 mL of QBT by gravity. The supernatant was entered to equilibrated QIAGEN-tip 500. The tip was washed two

times with 30 mL Buffer QC after the supernatant. The warm elution buffer was added and collected in 15 mL tube with 10 µl of DNAse free water in 1mL DNase free tube (Qiagen endotoxin-free MAXI PREP) and frozen in – 80 °C. Oligomers were inserted into miR30 in the vector construct.

Table 1. Oligomer sequences and target genes. The left row shows the name of each oligomer and the middle row gives the target genes and the right row gives the sequence of each oligomer.

oligomer	Target gene	Oligomer sequence
TRCN0000247096 '5UTR	CCM3/PDCD10	GTAATGAGCTAGAACGAGTAAA TTTACTCGTTCTAGCTCATTAA
TRCN0000144228 '3UTR	CCM3/PDCD10	TCAGGATGTTGAATGGGATTAT ATAATCCCATTCAACATCCTGG
TRCN0000140317_CDS	CCM3/PDCD10	CCGTAAGTGCCAACCGACTAAT ATTAGTCGGTTGGCACTTACGA
TRCN0000253692	HEG1	AGATCTCAGAGGCGGATCTTTA TAAAGATCCGCCTCTGAGATCC
TRCN0000253693	HEG1	CACCTTCGTGACAGAGTTTAAA TTTAAACTCTGTCACGAAGGTT
SIGMA_TRCN0000253690	HEG1	ATTCCGTATGGAGTGGATTAAG CTTAATCCACTCCATACGGAAG
TRCN0000072879	KRIT1	CCGGGTAGATAAAGTGGTAATA TATTACCACTTTATCTACCCGA
TRCN0000072880	KRIT1	TCCAGTCTCAATTCTCGGGAAT ATTCCCGAGAATTGAGACTGGC
TRCN0000105937	KRIT1	TCCTGTGTATGTAGGAGTGAAT ATTCACTCCTACATACACAGGG
SIGMA_ TRCN0000291592	KRIT1	CGCCTTGGATAAGTGGTTAGAT ATCTAACCACTTATCCAAGGCT

2.10. Viral delivery of CCM3 microRNA to hCMEC/D3 endothelial cells

hCMEC/D3 cells were prepared on collage-coat 6 well plate and infected with miRNA-TRCN0000247096 '5UTR , TRCN0000144228 '3UTR , TRCN0000140317_CDS (Table 1), control with random miRNA produced at 2.3 and 2.4. To activate promoter for dsRED of the construct, tetracycline was added to the cells for 7 days.

2.11. Flow Cytometry to select RNAi positive cells with RFP

The cells were trypsinized and washed (Method 2.2). The pellet was resuspended in 0.2 % BSA in PBS solution. The resuspension was filtered with 10-micron cell strainer. DsRed and Venus double positive D3 miR CCM3 were selected with BD FACSAria II SORP (High speed, 13-color, 4-laser cell Sorter) by Dennis Young (UCSD Moore Cancer center). The selected population were resuspended in 500 µl of fetal bovine serum with 1:100 anti-mycotic (CORE).

2.12. dsRed positive cell co-culture with HUVEC

The dsRed positive cells in serum were added to pre-seeded HUVEC population with anti-mycotic in 1 in 100 with HUVEC media (Method 2.2). After 24 hours, the fresh media with anti-mycotic was added (Method 2.2). After 72 hours, 0.5 µg/mL puromycin was added to induce drug efflux pump in D3 cells. After 96 hours, 1.0 µg/mL puromycin was added. The media was changed every 24 hours after adding puromycin. After 240 hours, the cells were taken off from puromycin treatment and doxycycline was added to activate the dsRED construct. The purified population using puromycin was re-selected using BD FACSAria II SORP (Method 2.12).

2.13. Coverslip placement and morphology characterization of RNAi cell line.

Sterile autoclaved coverslips were placed in 24 well plate. The resuspended cells (Method 2.3) were placed on the coverslips. As 2.8, the cells were fixed and immunostained.

2.14. HKi3 preparation and treatment of Wild type D3 cells

KRIT1 FERM domain-Rap 1b complex were purified and crystallized at room temperature with the reservoir solution (20-25% PEG 3,350, 100 mM Tris, pH 8.5, 100 mM

KCl) for a week. KRIT1-FERM domain-Rap 1b complex was diluted in DMSO to 10 mM (HKi3). HKi3 solution was diluted to 50 μM in D3 media. The cells were treated with 50 μM of HKi3, 50 μM of DMSO, PI3K inhibitor and VEGF. The cells were treated when they were 90 % confluent. The treatment was for 30 minutes. Then, the cells were lysed in 300 μl of cold lysis buffer (4 mL lysis buffer and 1 tablet of protease inhibitor and 1 tablet of phosphatase inhibitor) and stored in – 80 °C. For western blot, the 2.7. was repeated. Instead of 10 % milk in PBS, the membrane was blocked with 10 % BSA in PBS.

2.15. Immunoprecipitation.

Lysis buffer (20 mMTris, 150 mM NaCl, pH 7.4 containing 0.01% NP-40, and 1mM EDTA) was used to wash SPHERO Neutravidin Polystyrene Particles (Spherotech). The beads mixed with lysis buffer was incubated with reaction buffer at room temperature for 30 minutes (20 mM

Tris, 150 mM NaCl, pH 7.4 0.01% NP-40, 1mM EDTA, 1mM DTT, and 0.1% BSA). The beads were centrifuged and washed three times with cold reaction buffer. The samples were left on a rotator at 4 °C for 1 hour. The defrosted samples were centrifuged at max speed for 15 minutes. 30 μl of beads were added to the tube and washed three times with 300 μl of lysis buffer by spinning at 4000 g for 2 minutes at 4 C. The beads were incubated with 4 μg of p-PI3K antibody at 4 C on the rotator (mouse monoclonal p85 Millipore 05-212). The same process was repeated for PI3K and p-AKT and AKT antibody. The cell lysate was added to beads and incubated at 4 C on rotator for 1 hour. The samples were centrifuged at 4000 g for 2 minutes at 4 C and the supernatant was collected. They were washed 3 times with 300 μl of lysis buffer and inhibitors (25 mM Tris, pH 7.5, 200 mM NaCl, 1% Triton X-100, 0.5% Sodium

Inhibitor) and aspirated to 100 μl.

2.17 Western Blot of phosphorylated proteins.

The cells treated with HKi 003 at 2.15 were lysed with lysis buffer (25 mM Tris, pH 7.5, 200 mM NaCl, 1% Triton X-100, 0.5% Sodium Deoxycholate, 2.5X protease inhibitor, 2.5x PhosSTOP). The proteins collected from 2.16 and the supernatant from 2.16 were analyzed with Western Blot as 2. 7. The membrane was stained twice with phospho-antibodies and non-phospho antibodies. Antibodies used were listed: phospho-Akt-Ser473 (clone: 193H12; rabbit mAb; #4058; 1:250; Cell Signaling), Akt (clone: 40D4; mouse mAb; #2920; 1:500; Cell Signaling), phospho-PI3 Kinase p85 Tyr458 (rabbit polyclonal; #4228; 1:500; Cell Signaling). Antibody to PI3 Kinase, p85 (clone AB6; mouse mAb; #05-212; 1:250; EMD Millipore). Immunoprecipitated phosphoproteins was normalized to the total proteins for band intensity analysis. The activity of PI3K was measured as ration between the levels of total PI3K and levels of phospho-PI3KTyr^{458}. The activity of AKT was measured similarly by comparing with phosphor-AktSer^{473}

3. Results

3.1. Disruption of the HEG1-KRIT1 interaction by HKi3 triggers elevation of PI3K/AKT signaling in endothelial cells.

To investigate the effects of acute inhibition of the endothelial HEG1-KRIT1 interaction, we used the human cerebral microvascular endothelial cell-line, hCMEC/D3. Loss of endothelial *Krit1* or *Heg1* increases the expression of KLF2 and KLF4 transcription factors (Nowak et al., 2010 & Lopez-Ramirez et al., 2017 & Bharadwaj et al., 2010 & Cuttano et al., 2015 & Zhou et al., 2016). Therefore, we first assessed the level of the phosphoinositide 3-kinase (PI3K)/Akt signaling pathway previously implicated in the regulation of endothelial KLFs expression (Sako et al., 2008 & Huddleson et al., 2005 & Nayak et al., 2011). To this end, we first performed immunoprecipitation of PI3K using mouse monoclonal antibodies (methods 2.15), and activity was measure as the ratio between the levels of total PI3K and levels of phospho-PI3K-Tyr^{458} (methods 2.17). Total protein lysate obtained from hCMEC/D3 cells treated either with 50 μM small molecule HKi3 or vehicle for 1 h were analyzed. We observed that treatment with HKi3 induced a 2-fold increase in PI3K activity (Figure 6a). Furthermore, when hCMEC/D3 cells were treated with HKi3 we also observed a 2.2-fold increase in Akt activation, as assessed by Western blot analysis of phosphor-Akt-S^{473} (Figure 6b). These results suggest that disruption of the endothelial HEG1-KRIT1 protein complex using HKi3 increased PI3K activity that triggers AKT activation.

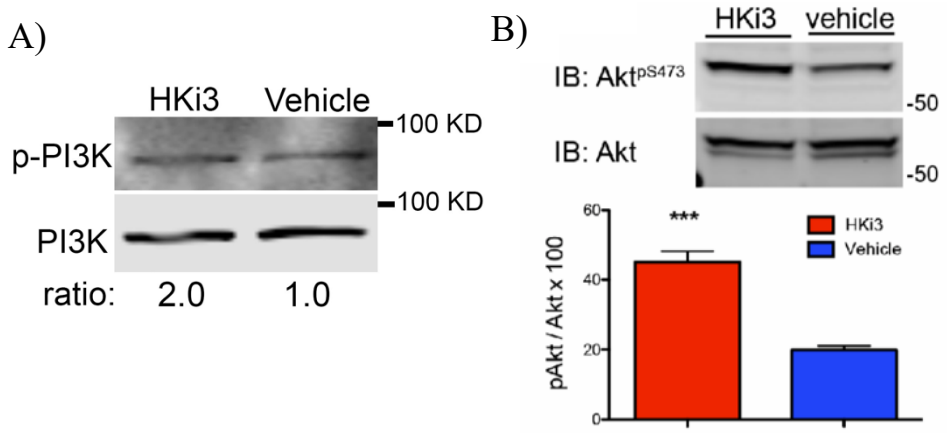

Figure 6. Hki3 treatment increases PI3K/AKT signaling pathway in hCMEC/D3 cell-line. hCMEC/D3 treated with Hki3 or DMSO. A) shows comparison of both phosphorylated PI3K and overall PI3K protein levels. B) shows comparison of both phosphorylated AKT and overall AKT protein level. Two-tailed t-test was performed. *** indicates that $p < 0.001$. The graph represents the protein level relative to the vehicle control.

3.2. HKi3 increases KLF2 and KLF4 mRNA levels in hCMEC/D3 cells

As mentioned in 3.1, genetic inactivation or knockdown of endothelial HEG1 or KRIT1 leads to the upregulation of KLF2 and KLF4 mRNA levels. However, it is unknown if the pharmacological inhibition of HEG1-KRIT1 protein interaction is sufficient to regulate the expression of KLF2 and KLF4 in endothelial cells. In order to evaluate the effect of HKi3 on KLF2 and KLF4 expression in hCMEC/D3 cells, we performed RT-qPCR analysis of KLF2 and KLF4 mRNA expression levels using total RNA (methods 2.5). We observed that KLF4 mRNA levels were slightly reduced following treatment with 10 uM HKi3 for 12h. However, increasing the concentration of HKi3 increases KLF4 mRNA levels further when compared to control-treated cells (Figure 7a). Upregulation of KLF4 mRNA levels at 50 µM was found to be ~6.5 fold increase while using 25 µM was observed to be ~2.5 fold-increase (Figure 7a). Similar results were observed when determining the mRNA expression levels of KLF2 with the exception that lower concentrations of HKi3 did not affect KLF2 mRNA levels (Figure 7b). The

upregulation of KLF2 mRNA levels at 50 μM, was ~2.5 fold increase. At 25 μM, it showed only ~1.5 fold increase (Figure 7b). These results indicate that HKi3 induces changes in mRNA expression levels in transcription factors KLF4 and KLF2 in a dose-dependent manner, and with the maximal effect being observed using 50 μM of Hki3.

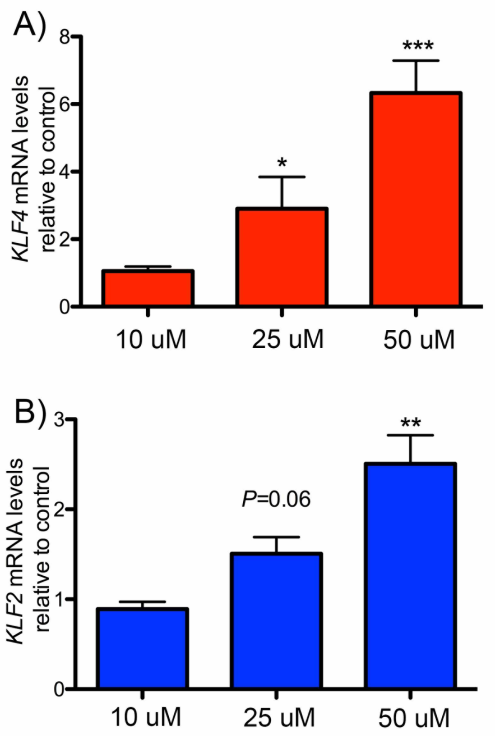

Figure 7. Dosage dependent KLF2/KLF4 mRNA increase with Hki3 treatment in hCMEC/D3. In A) B) cells were treated with Hki3 and DMSO with varying concentrations. KLF2/4 mRNA increased with higher Hki3 concentrations. Relative mRNA levels of experiments were shown as bars. 2-tailed t test was performed on the data. * represent $p < 0.05$. ** represents $p < 0.01$. *** represents $p < 0.001$.

From the data in Figure 3, we observed that a minimum 50 μM of HKi3 is effective in the upregulation of KLF2 and KLF4 in endothelial cells. To determine the effective treatment time for KLF2 and KLF4, we performed RT-qPCR analysis of KLF2 and KLF4 mRNA of expression levels using total RNA (methods 2.5). hCMEC/D3 cells were treated with 50 μM of HKi3 for 4 hs, 8 h, and 24 h (Fig 8a).

We observed that KLF4 mRNA levels were increased following treatment with 4 hours of HKi3 to ~4 fold. Increasing the treatment time of HKi3 increases KLF4 mRNA levels further when compared to control-treated cells (Figure 8a). The upregulation of KLF4 mRNA levels at 8 hours was observed to be ~2.5 fold increase, and an increase for 24 hours was observed to be ~6 fold-increase (Figure 8a). Similar results were observed when determining the mRNA expression levels of KLF2 (Figure 8b). Increasing the treatment time of HKi3 also increases KLF2 mRNA compared to the controls. The upregulation of KLF2 mRNA levels at 4 hours and 8 hours was similar to be ~1.5 and ~1.7 fold-increase (Figure 8b). Upregulation of KLF2 mRNA levels at 24 hours was observed to be ~2 fold increase. These results indicate that HKi3 induces changes in mRNA expression levels in transcription factors KLF4 and KLF2 in a time-dependent manner, and with the maximal effect being observed with 24 h of HKi3.

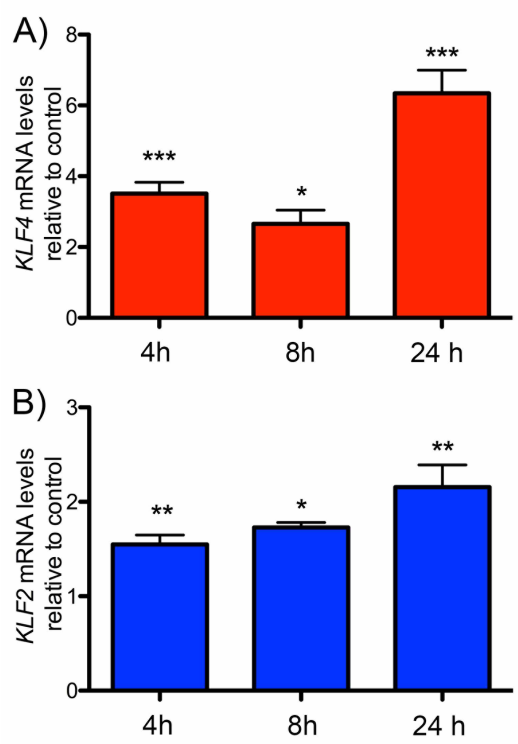

Figure 8. Time dependent KLF2/KLF4 mRNA increase with Hki3 treatment in hCMEC/D3.
E) shows KLF4 mRNA level changes with increasing time of Hki3 treatment. F) shows KLF2 mRNA level increase with increasing time of drug treatment. Relative mRNA levels of experiments were shown as bars. 2-tailed t test was performed on the data. * represent $p < 0.05$. ** represents $p < 0.01$. *** represents $p < 0.001$.

3.3. HKi3 increases KLF2 and KLF4 mRNA levels in HUVEC.

In an attempt to study the broad effect of HKi3 on endothelial cells, we repeated experiments using primary human umbilical vein endothelial cells (HUVECs). We observed that similar to hCMEC/D3 cells (microvascular cells), HUVEC-treated (large vein endothelial cells) with HKi3 for 24 hours showed upregulation of both KLF2 and KLF4 mRNA levels (Figure 9a, 7b).

To evaluate the effect of HKi3 on KLF2, and KLF4 expression in HUVEC cells, RT-qPCR analysis of KLF2 and KLF4 mRNA expression levels were performed using total RNA (methods 2.5). Similar patterns were observed in KLF4 mRNA level in both hCMEC/D3 cells and HUVEC in a dose-dependent manner. We observed that KLF4 mRNA levels were slightly

increased with treatment with 25 uM HKi3 for 24 hours to ~1.5 fold. Increasing the concentration of HKi3 increases KLF4 mRNA levels further when compared to control-treated cells (Figure 9a). The upregulation of KLF4 mRNA levels at 50 μM was observed to be ~6 fold increase while using 75 μM was observed to be ~8 fold-increase (Figure 9a). Similar results were observed when determining the mRNA expression levels of KLF2 except that 25 μM of HKi3 did not affect KLF2 mRNA levels (Figure 9b). Upregulation of KLF2 mRNA levels at 50 μM, was ~6 fold increase and at 75 μM, was ~8 fold. At 25 μM, KLF2 mRNA level did not change compared to the control (Figure 9b). These results indicate that HKi3 induces changes in HUVEC mRNA expression levels in transcription factors KLF4 and KLF2 in a dose-dependent manner, and with the maximal effect being observed using 75 μM of HKi3.

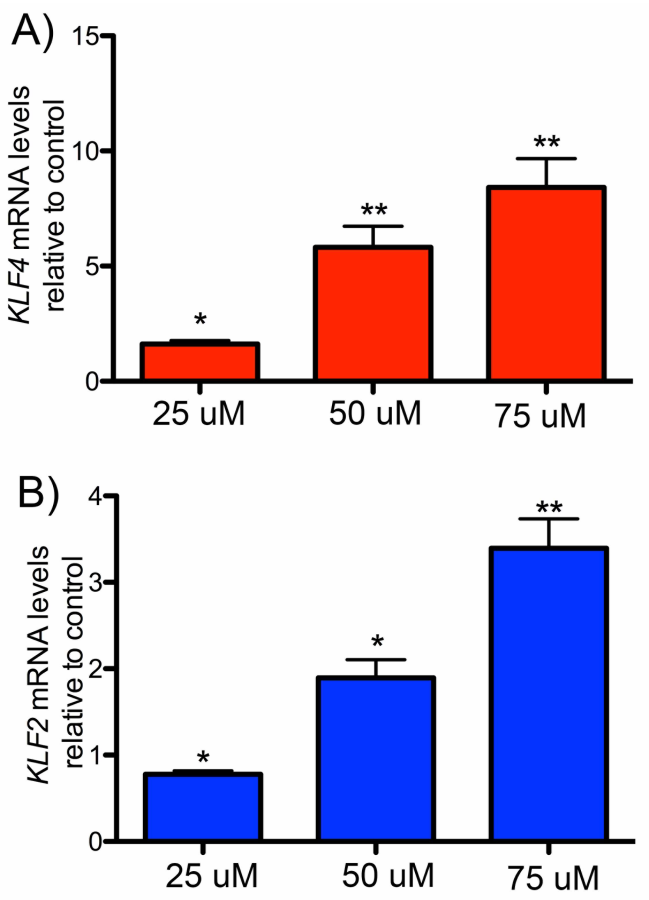

Figure 9. Dosage dependent KLF2/4 mRNA increases in HUVEC cells with HKi3 treatment.
A) shows KLF4 mRNA level change with increasing concentrations of HKi3. B) shows KLF2 mRNA level change with same concentrations of HKi3 as A). For 24 hours, HUVECs were incubated with doses indicated. Two tailed t-test was performed. * indicates $p < 0.05$. ** indicates $p < 0.01$. *** indicates $p < 0.001$. Bars show relative mRNA level compared to control.

3.5. Retrovirus transduction of tetracycline-regulated RNAi against *PDCD10* mRNA in hCMEC/D3 cell line

Loss of function of HEG1 or KRIT1 or PDCD10 (CCM genes) has been studied using RNA interference (RNAi) such as small interfering RNAs (siRNAs) and short hairpin RNAs (shRNA) directed against *HEG1* or *KRIT1* or *PDCD10* mRNA, respectively, in different vascular beds (hCMEC/D3 cells, HUVEC, bovine aortic endothelial cells, pulmonary artery endothelial cells among others) (DiStefano et al., 2014 & Lopez-Ramirez et al., 2019 & Chernaya et al., 2018). However, using these approaches are limited to short experimental duration (e.g., 3 to 4 days using siRNA) and the efficiency of transduction (e.g., transduction efficiency in hCMEC/D3 cells is 60%). Therefore, we adopted an inducible shRNA expression system (to knockdown CCM genes) that allow us to identify retroviral transduced cells and shRNA induction through the expression of two fluorescent reporters as previously reported (Zuber et al., 2019) (methods 2.8). This approach uses an inducible tetracycline-responsive element (TRE) promoter that control expression of a dsRed fluorescent protein and a microRNA-embedded shRNA directed against *PDCD10* (or other CCM genes) and a second promoter the phosphoglycerate kinase (PGK) that control the constitutive expression of the yellow-green fluorescent protein Venus (Zuber et al., 2019) that we denominated TRMPV-*PDCD10* (TRE-dsRed-miR30-against-PDCD10-PGK-Venus). Using this RNAi system, we generated stable hCMEC/D3 cells lines each expressing one of three different TRMPV-*PDCD10* constructs (methods 2.10). We observed that hCMEC/D3 cells transduced with retroviral particles of TRMPV-*PDCD10* in the presence of 2 µg/mL doxycycline for 7 days produce four populations of cell when analyzed by flow cytometry (Figure 10). We observed a large number of cells that were not transduced (~90% of the cells) and a small population of cell positive only to $dsRed^{+}$

(~0.2 % of cells) or only positive to Venus$^+$ (0.5% of cells, lack of shRNA induction) (Figure 10). We also observed a small population of cells positive to both dsRed$^+$ and Venus$^+$ (0.7 % of cells, relevant shRNA-expressing cell) (Figure 10). Using fluorescence-activated cell sorting (FACS) we sorted dsRed$^+$Venus$^+$ hCMEC/D3 and co-cultured them with HUVEC feeder cells to increase viability following FACS isolation. After one week in co-culture, hCMEC/D3 cells were selected by using 1.0 µg/mL puromycin.

Transduced hCMEC/D3 cells from the first sorting were subject to a second sorting were the population of dsRed$^+$Venus$^+$ hCMEC/D3 increased to ~16.5% (Figure 11). dsRed$^+$Venus$^+$ hCMEC/D3 cells from the second sorting were subject to co-cultured with HUVEC feeder cells and the processes repeated until we obtained ~ 60% dsRed$^+$Venus$^+$ hCMEC/D3 cells (data not shown) which are shRNA-expressing cell. These results show the feasibility to produce a human brain endothelial cell-line with stable expression of a tetracycline-regulated RNAi-directed against CCM genes.

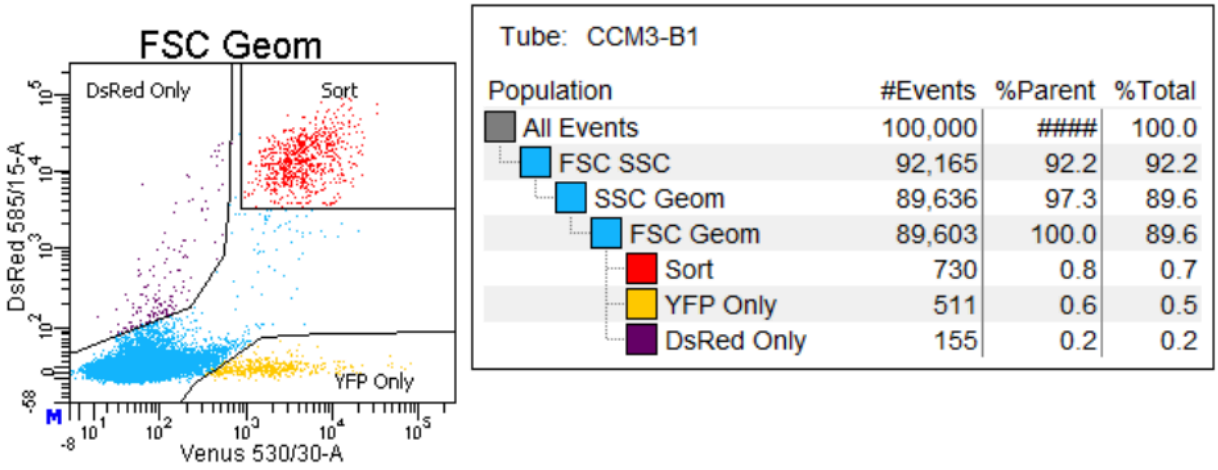

Figure 10. First sorting of TRMPV-*PDCD10*-hCMEC/D3.
hCMEC/D3 cells infected with miR was sorted via flow cytometry. Left graph shows the overall distribution of population by colors. The table on the right shows percentage distribution of each population. dsRED and VENUS double positive was represented as Red Sort population. dSRED and VENUS double positive population was 0.7 % total of 100,000 cells.

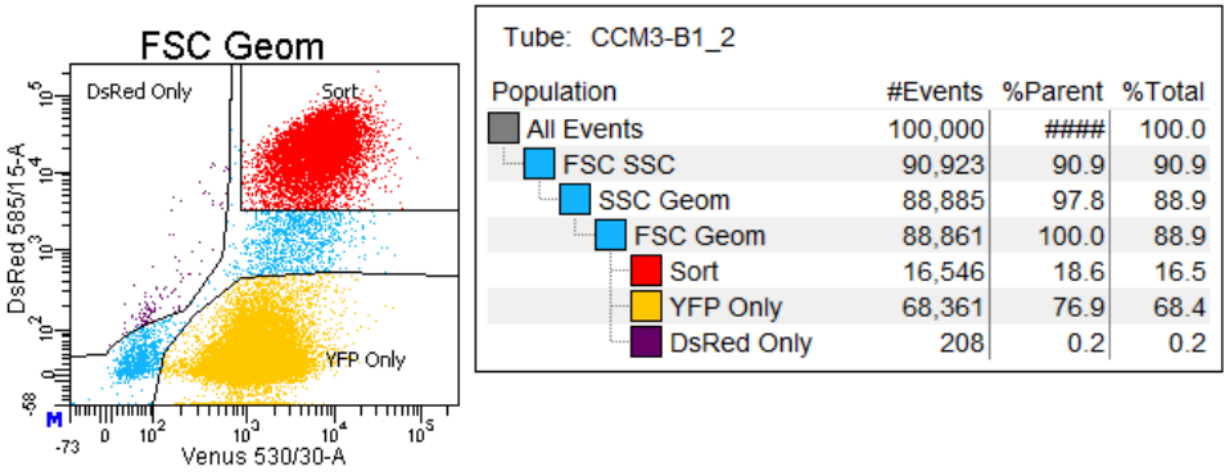

Figure 11. Second sorting of TRMPV-*PDCD10*-hCMEC/D3
hCMEC/D3 dsRED positive from Figure 12 was resorted via flow cytometry. The graph on the left shows the overall distribution of population by colors. The table on the right shows the percentage distribution of each population. dsRED and VENUS positive population was 16.5 % of total 100,000 cells.

3.7. Time-controlled knockdown of PDCD10 in hCMEC/D3 cells

We next investigated the phenotype and gene expression of hCMEC/D3 cells with stable expression of TRMPV-*PDCD10.* Since PDCD10 is known to regulate endothelial junctional integrity (Stamatovic et al., 2015), we examine the organization of intercellular junctions following the time-controlled knockdown of PDCD10 in TRMPV-*PDCD10*-hCMEC/D3 stable cells. We observed that TRMPV-*PDCD10*-hCMEC/D3 stable cells non-treated with doxycycline do not express dsRed protein and, therefore, lack of shRNA induction (Figure 12). In contrast, we observed that TRMPV-*PDCD10*-hCMEC/D3 doxycycline-treated cells showed robust expression of dsRed protein and therefore are shRNA-expressing cells (Figure 12). We next assessed junctional integrity by immunocytochemistry using antibodies against VE-cadherin. VE-cadherin staining in TRMPV-*PDCD10*-hCMEC/D3 vehicle-treated cells form a continuous peripheral belt at the cell-cell junctions (Figure 12). In contrast, TRMPV-*PDCD10*-hCMEC/D3

doxycycline-treated cells show marked disruption of VE-cadherin staining in the junctional belt (Fig 12). These results show that loss of PDCD10 in EC by time-controlled expression of ShRNA against *PDCD10* mRNA leads to changes in the continuity of junctional protein VE-cadherin.

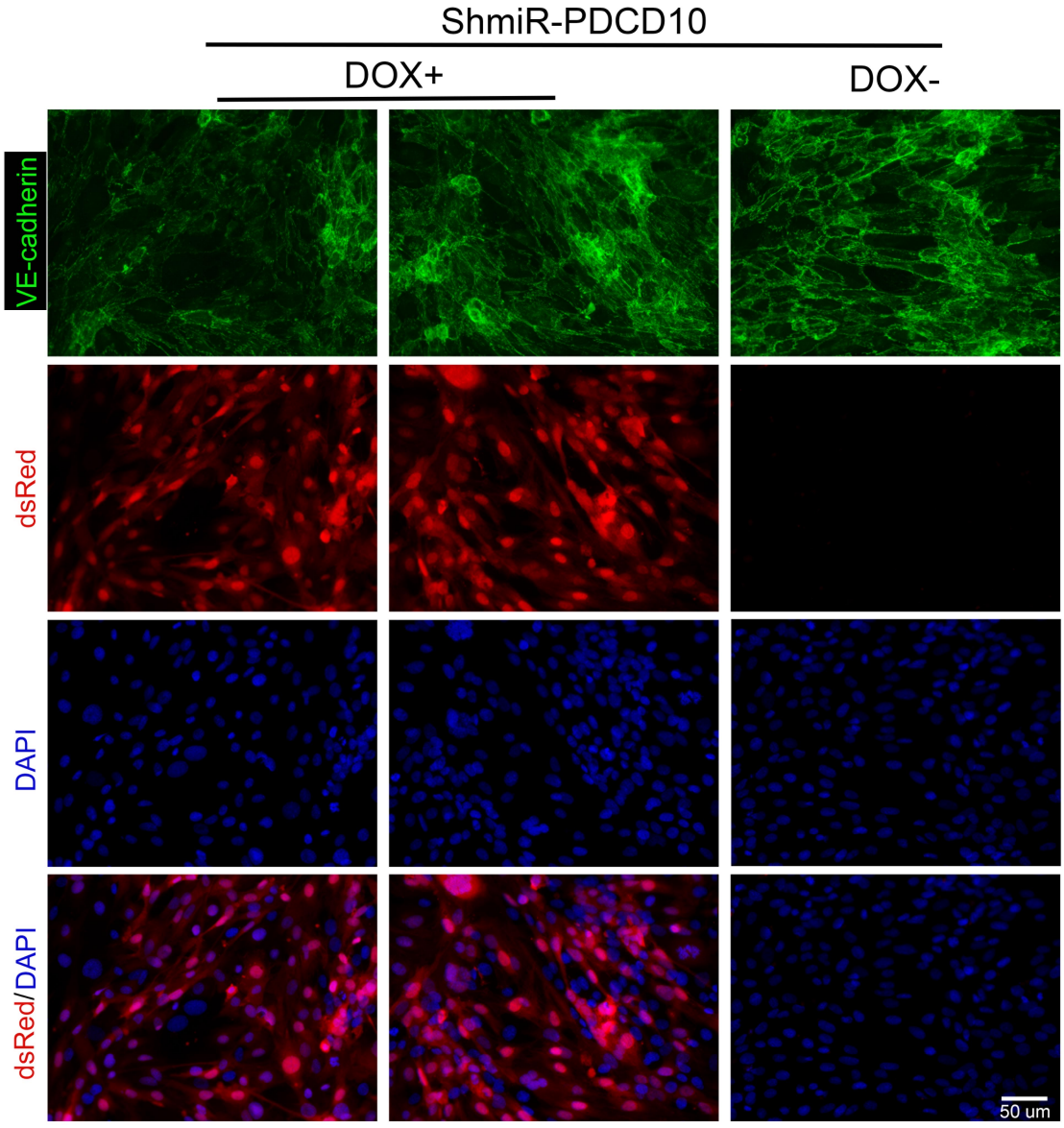

Figure 12. Morphology characteristics of TRMPV-*PDCD10*-hCMEC/D3. The left two columns are CCM3-miR-B1 with doxycycline. The right column is CCM3-miR-B1 without doxycycline. VE-cadherin at top was stained with green. dsRED and DAPI (blue) staining were overlapped in CCM3-miR-B1 with doxycycline. There was no dsRED observed in CCM3-miR-B1 without doxycycline.

3.8. CCM3-miRNA-B1 upregulated vasoprotective molecules: KLF2, KLF4, eNOS

We used RT-qPCR to validate that TRMPV-*PDCD10*-hCMEC/D3 decreased the expression of PDCD10 and increased expression of PDCD10 (KLF2, KLF4, eNOS) (Method 2.5). Transduced hCMEC/D3 cells that were sorted twice through FAC (Fig 11) were used. We previously reported that KLF2, KLF4, and eNOS increased after the loss of PDCD10 (Soliman, 2019). We observed that TRMPV-*PDCD10*-hCMEC/D3 increases KLF2, KLF4, and eNOS mRNA level but decreases the Pdcd10 mRNA level (Fig 13). This shows that PDCD10 knockdown was effective in TRMPV-*PDCD10*-hCMEC/D3 because PDCD10 inactivation led to an increase in KLF2, KLF4, eNOS, consistent with previous result (Soliman, 2019).

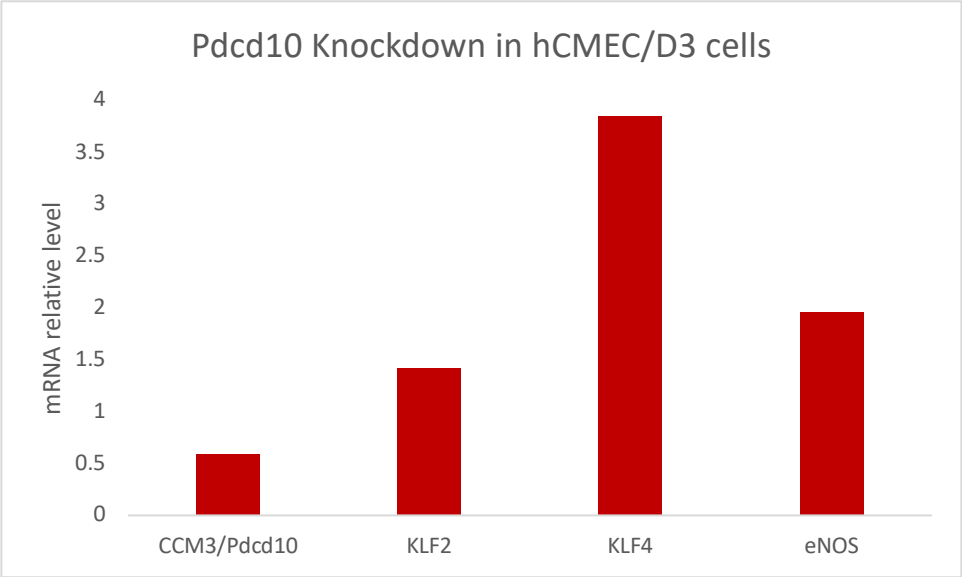

Figure 13. RT-qPCR results of TRMPV-*PDCD10*-hCMEC/D3. The gene levels in CCM3-miR-B1 cell lines sorted through flow cytometry were analyzed. CCM3 level dropped about 50 %. KLF2, KLF4 and eNOS showed increase in mRNA level.

The part of Chapter 3 and 4 of this thesis is currently submitted for publication.

4. Discussion

Loss of HEG1 or KRIT1 in endothelial cells leads to upregulation in KLF2 and KLF4 expression. However, it is still unclear if inhibition of HEG1-KRIT1 protein complex could also lead to similar effects in endothelial cells. In this research, I study the effects of HKi3, an small molecule, that disrupt HEG1-KRIT1 interaction to investigate downstream effects in endothelial cells.

We found that pharmacological inhibition of the HEG1-KRIT1 protein interaction can be used to study the signaling events regulated by this protein complex. Indeed, acute inhibition of the endothelial HEG1-KRIT1 interaction with HKi3 rapidly increases PI3K/Akt activity. Previous studies have shown that mechanotransduction via fluid shear stress mediates PI3K/Akt activation. PI3K/AKT signaling contributes to vasodilation through an increase in eNOS gene expression and activity (Huddleson et al., 2005 & Lee, 2014). Moreover, a recent study in zebrafish suggested that *heg1* and *krit1* expression confer cardiovascular development accuracy by fine-tuning endothelial cell response to blood flow (Donat et al., 2018). However, further research will be needed to investigate whether HEG1-KRIT1 protein complex is interconnected to mechanosensing proteins that regulate PI3K/Akt activation. In this context, Previous studies have shown that fluid shear stress increases tension on PECAM1 and subsequent activation of Src family kinases-induced ligand-independent VEGFR2/3 activation that, in turn, activates PI3K that precedes AKT phosphorylation (Coon et al., 2015 & Jin et al., 2005 & Baeyens et al., 2016). In addition, Rap1 protein has been proposed to be activated by laminar shear stress to promote the endothelial mechanosensing protein complex by increasing the association between PECAM1-VEGFR2-VE-cadherin and subsequent PI3K/Akt signaling (Lakshmikanthan et al., 2015). Importantly, Rap1 activity regulates the junctional localization of KRIT1 (Glading &

Ginsberg, 2010), and previous crystal structure analysis revealed that HEG1-KRIT1- Rap1 can form a ternary complex (Gingras et al., 2013). Therefore, future research should be focused on investigated whether HEG1-KRIT1 protein complex regulates PI3K/Akt signaling by interaction with mechanosensing proteins or by direct regulation in PI3K activity.

Our results demonstrate that pharmacological inhibition of the endothelial HEG1-KRIT1 interaction is sufficient to increase KLF4 and KLF2 expression in a dose- and time-dependent manner in endothelial cells. It is well documented that genetic inactivation or knockdown of endothelial HEG1 or KRIT1 results in the upregulation of KLF4 and KLF2, which are genes normally induced by laminar blood flow (Cuttano et al., 2015 & Bharadwaj et al., 2010 & Zhou et al., 2016 & Lopez-Ramirez et al., 2017 & Nowak et al., 2010 & Chistiakov et al., 2016 & Gore et al., 2012). Importantly, the gain of endothelial MEKK3 activity has been associated with the upregulation of KLF4 and KLF2 in the CCM disease (Cuttano et al., 2015 & Bharadwaj et al., 2010 & Zhou et al., 2016). MEKK3 interacts with the CCM protein complex by binding directly to CCM2 (17, 46), and loss of CCM proteins results in an increase in MEK5-ERK5-MEF2 mechanotransduction pathway (Cuttano et al., 2015 & Bharadwaj et al., 2010 & Chistiakov et al., 2016 & Zhou et al., 2016 & Gore et al., 2012 & Cullere et al., 2015) that has also been shown to contribute to the responsiveness of endothelial cells to laminar blood flow (Donat et al., 2018). Therefore, this study suggests that part of the effect of laminar shear stress can be mimic by small molecules such as HKi3 that disrupt the HEG1-KRIT1 interaction. Future studies should be designed to investigate whether the increase in KLF2 and KLF4 expression is directly regulated by PI3K/Akt signaling or by MEKK3 activity following acute inhibition of the endothelial HEG1-KRIT1 protein complex.

In this work, TRMPV-Pdcd10 cell line was developed as an approach to time-controlled gene expression of PDCD10/CCM3 in human endothelial cells. Initially, these experiments were designed to validate the specificity of HKi3 on human endothelial. These experiments consisted of evaluating the effects of HKi3 on KLF2/KLF4 expression and PI3K/Akt signaling following knockdown of genes part of the HEG1-KRIT1 protein complex. However, due to the timing, we were only able to characterize *PDCD10* knockdown in hCMEC/D3 cells. In the future, we will use the same strategy to time-controlled the HEG1 and KRIT1 gene expression using siRNA technology in hCMEC/D3 cells. Our results show that inhibition of Pdcd10 in TRMPV-Pdcd10 cells led to the disruption of endothelial cell-to-cell contacts and an increase in KLF2 and KLF4 gene expression. These results are consistent with previous work by time-controlled genetic inactivation of Pdcd10 in brain microvascular endothelial cells (Chernaya et al., 2018& Lopez-ramirez et al., 2019). Therefore, this study suggests that the HEG1-KRIT1 protein complex may be interconnected to mechanosensing proteins (e.g, PECAM1, VE-cadherin, and VEGFR2/3) that respond to flow-induced mechanotransduction (Coon et al., 2015 & DiStefano et al., 2014). Thus, novel HKi will provide new tools for analysis of the signaling events that follow the disruption of HEG1-KRIT1 interaction with previously inaccessible temporal precision.

The part of Chapter 3 and 4 of this thesis is currently submitted for publication.

References

Abe, J., & Berk, B. C. (2014). Novel mechanisms of endothelial Mechanotransduction. *Arteriosclerosis, Thrombosis, and Vascular Biology*, *34*(11), 2378-2386. https://doi.org/10.1161/atvbaha.114.303428

Arrieta-Blanco, J., Onate-Sanchez, R., Martinez-Lopez, F., Onate-Cabrerizo, D., & Cabrerizo-Merino, M. (2014). Inherited, congenital and acquired disorders by hemostasis (vascular, platelet and plasmatic phases) with repercussions in the therapeutic oral sphere. *Medicina Oral Patología Oral y Cirugia Bucal*, e280-e288. https://doi.org/10.4317/medoral.19560

Baeyens, N., Bandyopadhyay, C., Coon, B. G., Yun, S., & Schwartz, M. A. (2016). Endothelial fluid shear stress sensing in vascular health and disease. *Journal of Clinical Investigation*, *126*(3), 821-828. https://doi.org/10.1172/jci83083

Bazzoni, G., & Dejana, E. (2004). Endothelial cell-to-cell junctions: Molecular organization and role in vascular homeostasis. *Physiological Reviews*, *84*(3), 869-901. https://doi.org/10.1152/physrev.00035.2003

Bergers, G., & Song, S. (2005). The role of pericytes in blood-vessel formation and maintenance. *Neuro-Oncology*, *7*(4), 452-464. https://doi.org/10.1215/s1152851705000232

Bharadwaj, A. S., Kelly, M., Kim, D., & Chao, H. (2010). Induction of immune tolerance to FIX by intramuscular AAV gene transfer is independent of the activation status of dendritic cells. *Blood*, *115*(3), 500-509. https://doi.org/10.1182/blood-2009-08-239509

Biswas, I., & A. Khan, G. (2019). Endothelial dysfunction in cardiovascular diseases. *Microcirculation [Working Title]*. https://doi.org/10.5772/intechopen.89365

Carmona, G., Göttig, S., Orlandi, A., Scheele, J., Bäuerle, T., Jugold, M., Kiessling, F., Henschler, R., Zeiher, A. M., Dimmeler, S., & Chavakis, E. (2009). Role of the small GTPase Rap1 for integrin activity regulation in endothelial cells and angiogenesis. *Blood*, *113*(2), 488-497. https://doi.org/10.1182/blood-2008-02-138438

Chatterjee, S., & Fisher, A. B. (2014). Mechanotransduction in the endothelium: Role of membrane proteins and reactive oxygen species in sensing, transduction, and transmission of the signal with altered blood flow. *Antioxidants & Redox Signaling*, *20*(6), 899-913. https://doi.org/10.1089/ars.2013.5624

Chernaya, O., Zhurikhina, A., Hladyshau, S., Pilcher, W., Young, K. M., Ortner, J., Andra, V., Sulchek, T. A., & Tsygankov, D. (2018). Biomechanics of endothelial tubule formation differentially modulated by cerebral cavernous malformation proteins. *iScience*, *9*, 347-358. https://doi.org/10.1016/j.isci.2018.11.001

Chiplunkar, A. R., Curtis, B. C., Eades, G. L., Kane, M. S., Fox, S. J., Haar, J. L., & Lloyd, J. A. (2013). The krüppel-like factor 2 and krüppel-like factor 4 genes interact to maintain endothelial integrity in mouse embryonic vasculogenesis. *BMC Developmental Biology*, *13*(1), 40. https://doi.org/10.1186/1471-213x-13-40

Chistiakov, D. A., Orekhov, A. N., & Bobryshev, Y. V. (2016). Effects of shear stress on endothelial cells: Go with the flow. *Acta Physiologica*, *219*(2), 382-408. https://doi.org/10.1111/apha.12725

Chiu, J., & Chien, S. (2011). Effects of disturbed flow on vascular endothelium: Pathophysiological basis and clinical perspectives. *Physiological Reviews*, *91*(1), 327-387. https://doi.org/10.1152/physrev.00047.2009

CLARK, P. R., JENSEN, T. J., KLUGER, M. S., MORELOCK, M., HANIDU, A., QI, Z., TATAKE, R. J., & POBER, J. S. (2011). MEK5 is activated by shear stress, activates ERK5 and induces KLF4 to modulate TNF responses in human dermal Microvascular endothelial cells. *Microcirculation*, *18*(2), 102-117. https://doi.org/10.1111/j.1549-8719.2010.00071.x

Coon, B. G., Baeyens, N., Han, J., Budatha, M., Ross, T. D., Fang, J. S., Yun, S., Thomas, J., & Schwartz, M. A. (2015). Intramembrane binding of VE-cadherin to VEGFR2 and VEGFR3 assembles the endothelial mechanosensory complex. *The Journal of General Physiology*, *145*(4), 1454OIA13. https://doi.org/10.1085/jgp.1454oia13

Cullere, X., Plovie, E., Bennett, P. M., MacRae, C. A., & Mayadas, T. N. (2015). The cerebral cavernous malformation proteins CCM2L and CCM2 prevent the activation of the MAP kinase MEKK3. *Proceedings of the National Academy of Sciences*, *112*(46), 14284-14289. https://doi.org/10.1073/pnas.1510495112

Cuttano, R., Rudini, N., Bravi, L., Corada, M., Giampietro, C., Papa, E., Morini, M. F., Maddaluno, L., Baeyens, N., Adams, R. H., Jain, M. K., Owens, G. K., Schwartz, M., Lampugnani, M. G., & Dejana, E. (2015). KLF 4 is a key determinant in the development and progression of cerebral cavernous malformations. *EMBO Molecular Medicine*, *8*(1), 6-24. https://doi.org/10.15252/emmm.201505433

Daneman, R., & Prat, A. (2015). The Blood–Brain Barrier. *Cold Spring Harb Perspectives in Biology*, *7*(1). https://doi.org/10.1101/cshperspect.a020412

Davis, G. E., & Senger, D. R. (2005). Endothelial Extracellular matrix. *Circulation Research*, *97*(11), 1093-1107. https://doi.org/10.1161/01.res.0000191547.64391.e3

De Kreuk, B., Gingras, A. R., Knight, J. D., Liu, J. J., Gingras, A., & Ginsberg, M. H. (2015). Author response: Heart of glass anchors Rasip1 at endothelial cell-cell junctions to support vascular integrity. https://doi.org/10.7554/elife.11394.022

Dejana, E., & Orsenigo, F. (2013). Endothelial adherens junctions at a glance. *Journal of Cell Science*, *126*(12), 2545-2549. https://doi.org/10.1242/jcs.124529

DiStefano, P. V., Kuebel, J. M., Sarelius, I. H., & Glading, A. J. (2014). KRIT1 protein depletion modifies endothelial cell behavior via increased vascular endothelial growth factor (VEGF) signaling. *Journal of Biological Chemistry*, *289*(47), 33054-33065. https://doi.org/10.1074/jbc.m114.582304

Donat, S., Lourenço, M., Paolini, A., Otten, C., Renz, M., & Abdelilah-Seyfried, S. (2018). Heg1 and Ccm1/2 proteins control endocardial mechanosensitivity during zebrafish valvulogenesis. *eLife*, *7*. https://doi.org/10.7554/elife.28939

Fan, Y., Lu, H., Liang, W., Hu, W., Zhang, J., & Chen, Y. (2017). Krüppel-like factors and vascular wall homeostasis. *Journal of Molecular Cell Biology*, *9*(5), 352–363. https://doi.org/10.1093/jmcb/mjx037

Fisher, O. S., Liu, W., Zhang, R., Stiegler, A. L., Ghedia, S., Weber, J. L., & Boggon, T. J. (2014). Structural basis for the disruption of the cerebral cavernous malformations 2 (CCM2) interaction with Krev interaction trapped 1 (KRIT1) by disease-associated mutations. *Journal of Biological Chemistry*, *290*(5), 2842-2853. https://doi.org/10.1074/jbc.m114.616433

Fukuhara, S., Sakurai, A., Sano, H., Yamagishi, A., Somekawa, S., Takakura, N., Saito, Y., Kangawa, K., & Mochizuki, N. (2005). Cyclic AMP potentiates vascular endothelial cadherin-mediated cell-cell contact to enhance endothelial barrier function through an epac-rap1 signaling pathway. *Molecular and Cellular Biology*, *25*(1), 136-146. https://doi.org/10.1128/mcb.25.1.136-146.2005

Förster, C. (2008). Tight junctions and the modulation of barrier function in disease. *Histochemistry and Cell Biology*, *130*(1), 55-70. https://doi.org/10.1007/s00418-008-0424-9

Gill, S. E., Rohan, M., & Mehta, S. (2015). Role of pulmonary microvascular endothelial cell apoptosis in murine sepsis-induced lung injury in vivo. *Respiratory Research*, *16*(1). https://doi.org/10.1186/s12931-015-0266-7

Gingras, A. R., Liu, J. J., & Ginsberg, M. H. (2012). Structural basis of the junctional Anchorage of the cerebral cavernous malformations complex. *The Journal of Cell Biology*, *199*(1), 39-48. https://doi.org/10.1083/jcb.201205109

Gingras, A. R., Puzon-McLaughlin, W., & Ginsberg, M. H. (2013). The structure of the ternary complex of Krev interaction trapped 1 (KRIT1) bound to both the Rap1 GTPase and the heart of glass (HEG1) cytoplasmic tail. *Journal of Biological Chemistry*, *288*(33), 23639-23649. https://doi.org/10.1074/jbc.m113.462911

Glading, A. J., & Ginsberg, M. H. (2010). Rap1 and its effector KRIT1/CCM1 regulate -catenin signaling. *Journal of Cell Science*, *123*(3), e1-e1. https://doi.org/10.1242/jcs.067728

Gomez, N., Erazo, T., & Lizcano, J. M. (2016). ERK5 and cell proliferation: Nuclear localization is what matters. *Frontiers in Cell and Developmental Biology*, *4*. https://doi.org/10.3389/fcell.2016.00105

Gore, A. V., Monzo, K., Cha, Y. R., Pan, W., & Weinstein, B. M. (2012). Vascular development in the zebrafish. *Cold Spring Harbor perspectives in medicine 2*. https://doi.org/10.1101/cshperspect.a006684

Gunel, M., Laurans, M. S., Shin, D., DiLuna, M. L., Voorhees, J., Choate, K., Nelson-Williams, C., & Lifton, R. P. (2002). KRIT1, a gene mutated in cerebral cavernous malformation, encodes a microtubule-associated protein. *Proceedings of the National Academy of Sciences*, *99*(16), 10677-10682. https://doi.org/10.1073/pnas.122354499

Hahn, C., & Schwartz, M. A. (2009). Mechanotransduction in vascular physiology and atherogenesis. *Nature Reviews Molecular Cell Biology*, *10*(1), 53-62. https://doi.org/10.1038/nrm2596

Hogan, B. M., Bussmann, J., Wolburg, H., & Schulte-Merker, S. (2008). Ccm1 cell autonomously regulates endothelial cellular morphogenesis and vascular tubulogenesis in zebrafish. *Human Molecular Genetics*, *17*(16), 2424-2432. https://doi.org/10.1093/hmg/ddn142

Huddleson, J. P., Ahmad, N., Srinivasan, S., & Lingrel, J. B. (2005). Induction of KLF2 by fluid shear stress requires a novel promoter element activated by a Phosphatidylinositol 3-Kinase-dependent chromatin-remodeling pathway. *Journal of Biological Chemistry*, *280*(24), 23371-23379. https://doi.org/10.1074/jbc.m413839200

Jin, Z., Ueba, H., Tanimoto, T., Lungu, A. O., Frame, M. D., & Berk, B. C. (2003). Ligand-independent activation of vascular endothelial growth factor receptor 2 by fluid shear stress regulates activation of endothelial nitric oxide Synthase. *Circulation Research*, *93*(4), 354-363. https://doi.org/10.1161/01.res.0000089257.94002.96

Jin, Z., Wong, C., Wu, J., & Berk, B. C. (2005). Flow shear stress stimulates Gab1 tyrosine phosphorylation to mediate protein kinase B and endothelial nitric-oxide Synthase activation in endothelial cells. *Journal of Biological Chemistry*, *280*(13), 12305-12309. https://doi.org/10.1074/jbc.m500294200

Kawasaki, K., Smith, R. S., Hsieh, C., Sun, J., Chao, J., & Liao, J. K. (2003). Activation of the Phosphatidylinositol 3-Kinase/Protein kinase Akt pathway mediates nitric oxide-induced endothelial cell migration and angiogenesis. *Molecular and Cellular Biology*, *23*(16), 5726-5737. https://doi.org/10.1128/mcb.23.16.5726-5737.2003

Kim, C. W., Pokutta-Paskaleva, A., Kumar, S., Timmins, L. H., Morris, A. D., Kang, D., Dalal, S., Chadid, T., Kuo, K. M., Raykin, J., Li, H., Yanagisawa, H., Gleason, R. L., Jo, H., & Brewster, L. P. (2017). Disturbed flow promotes arterial stiffening through thrombospondin-1. *Circulation*, *136*(13), 1217-1232. https://doi.org/10.1161/circulationaha.116.026361

Klabunde, R. E. (2017). [drawing]. Cardiovascular Physiology Concepts. https://www.cvphysiology.com/Blood%20Pressure/BP019

Kleaveland, B., Zheng, X., Liu, J. J., Blum, Y., Tung, J. J., Zou, Z., Sweeney, S. M., Chen, M., Guo, L., Lu, M., Zhou, D., Kitajewski, J., Affolter, M., Ginsberg, M. H., & Kahn, M. L. (2009). Regulation of cardiovascular development and integrity by the heart of glass–cerebral cavernous malformation protein pathway. *Nature Medicine*, *15*(2), 169-176. https://doi.org/10.1038/nm.1918

Komarova, Y. A., Kruse, K., Mehta, D., & Malik, A. B. (2017). Protein interactions at endothelial junctions and signaling mechanisms regulating endothelial permeability. *Circulation Research*, *120*(1), 179-206. https://doi.org/10.1161/circresaha.116.306534

Kooistra, M. R., Dube, N., & Bos, J. L. (2006). Rap1: A key regulator in cell-cell Junction formation. *Journal of Cell Science*, *120*(1), 17-22. https://doi.org/10.1242/jcs.03306

Lakshmikanthan, S., Zheng, X., Nishijima, Y., Sobczak, M., Szabo, A., Vasquez-Vivar, J., Zhang, D. X., & Chrzanowska-Wodnicka, M. (2015). Rap1 promotes endothelial mechanosensing complex formation, NO release and normal endothelial function. *EMBO reports*, *16*(5), 628-637. https://doi.org/10.15252/embr.201439846

Lee, M. Y., Luciano, A. K., Ackah, E., Rodriguez-Vita, J., Bancroft, T. A., Eichmann, A., Simons, M., Kyriakides, T. R., Morales-Ruiz, M., & Sessa, W. C. (2014). Endothelial Akt1 mediates angiogenesis by phosphorylating multiple angiogenic substrates. *Proceedings of the National Academy of Sciences*, *111*(35), 12865-12870. https://doi.org/10.1073/pnas.1408472111

Li, X., Zhang, R., Draheim, K. M., Liu, W., Calderwood, D. A., & Boggon, T. J. (2012). Structural basis for small G protein effector interaction of ras-related protein 1 (Rap1) and adaptor protein Krev interaction trapped 1 (KRIT1). *Journal of Biological Chemistry*, *287*(26), 22317-22327. https://doi.org/10.1074/jbc.m112.361295

Lopez-Ramirez, M. A., Fonseca, G., Zeineddine, H. A., Girard, R., Moore, T., Pham, A., Cao, Y., Shenkar, R., De Kreuk, B., Lagarrigue, F., Lawler, J., Glass, C. K., Awad, I. A., & Ginsberg, M. H. (2017). Thrombospondin1 (TSP1) replacement prevents cerebral cavernous malformations. *Journal of Experimental Medicine*, *214*(11), 3331-3346. https://doi.org/10.1084/jem.20171178

Lopez-Ramirez, M. A., Haynes, M. K., Hale, P., Oukoloff, K., Bautista, M., Gongol, B., Shyy, J. Y., Ballatore, C., Sklar, L. A., & Gingras, A. R. (2019). Pharmacological inhibition of the heart of glass (heg1)-krev interaction trapped protein 1 (KRIT1) protein complex increases krüppel-like factors 4 and 2 (KLF4/2) expression in endothelial cells. https://doi.org/10.1101/744821

Lopez-Ramirez, M. A., Pham, A., Girard, R., Wyseure, T., Hale, P., Yamashita, A., Koskimäki, J., Polster, S., Saadat, L., Romero, I. A., Esmon, C. T., Lagarrigue, F., Awad, I. A., Mosnier, L. O., & Ginsberg, M. H. (2019). Cerebral cavernous malformations form an anticoagulant vascular domain in humans and mice. *Blood*, *133*(3), 193-204. https://doi.org/10.1182/blood-2018-06-856062

Lopez-Ramirez, M. A., Wu, D., Pryce, G., Simpson, J. E., Reijerkerk, A., King-Robson, J., Kay, O., Vries, H. E., Hirst, M. C., Sharrack, B., Baker, D., Male, D. K., Michael, G. J., & Romero, I. A. (2014). Microrna-155 negatively affects blood–brain barrier function during neuroinflammation. *The FASEB Journal*, *28*(6), 2551-2565. https://doi.org/10.1096/fj.13-248880

Mably, J. D., Burns, C., Chen, J., Fishman, M. C., & Mohideen, M. P. (2003). Heart of glass regulates the concentric growth of the heart in Zebrafish. *Current Biology*, *13*(24), 2138-2147. https://doi.org/10.1016/j.cub.2003.11.055

Mably, J. D., Chuang, L. P., Serluca, F. C., Mohideen, M. A., Chen, J. N., & Fishman, M. C. (2006). Santa and Valentine pattern concentric growth of cardiac myocardium in the zebrafish. *Development*, *133*(16), 3139-3146. https://doi.org/10.1242/dev.02469

Mazurek, R., Dave, J., Chandran, R., Misra, A., Sheikh, A., & Greif, D. (2017). Vascular cells in blood vessel wall development and disease. *Advances in Pharmacology*, 323-350. https://doi.org/10.1016/bs.apha.2016.08.001

Michiels, C. (2003). Endothelial cell functions. *Journal of Cellular Physiology*, *196*(3), 430-443. https://doi.org/10.1002/jcp.10333

Murray, I. R., Baily, J. E., Chen, W. C., Dar, A., Gonzalez, Z. N., Jensen, A. R., Petrigliano, F. A., Deb, A., & Henderson, N. C. (2017). Skeletal and cardiac muscle pericytes: Functions and therapeutic potential. *Pharmacology & Therapeutics*, *171*, 65-74. https://doi.org/10.1016/j.pharmthera.2016.09.005

Müller, B., Lang, S., Dominietto, M., Rudin, M., Schulz, G., Deyhle, H., Germann, M., Pfeiffer, F., David, C., & Weitkamp, T. (2008). High-resolution tomographic imaging of microvessels. *Developments in X-Ray Tomography VI*. https://doi.org/10.1117/12.794157

Nayak, L., Lin, Z., & Jain, M. K. (2011). "Go with the flow": How krüppel-like factor 2 regulates the Vasoprotective effects of shear stress. *Antioxidants & Redox Signaling*, *15*(5), 1449-1461. https://doi.org/10.1089/ars.2010.3647

Newman, P. J., & Newman, D. K. (2003). Signal transduction pathways mediated by PECAM-1. *Arteriosclerosis, Thrombosis, and Vascular Biology*, *23*(6), 953-964. https://doi.org/10.1161/01.atv.0000071347.69358.d9

Noguchi, N., & Jo, H. (2011). Redox going with vascular shear stress. *Antioxidants & Redox Signaling*, *15*(5), 1367-1368. https://doi.org/10.1089/ars.2011.4011

Nowak, D., Ogawa, S., Müschen, M., Kato, M., Kawamata, N., Meixel, A., Nowak, V., Kim, H. S., Kang, S., Paquette, R., Chang, M., Thoennissen, N. H., Mossner, M., Hofmann, W., Kohlmann, A., Weiss, T., Haferlach, T., Haferlach, C., & Koeffler, H. P. (2010). SNP array analysis of tyrosine kinase inhibitor-resistant chronic myeloid leukemia identifies heterogeneous secondary genomic alterations. *Blood*, *115*(5), 1049-1053. https://doi.org/10.1182/blood-2009-03-210377

Okamoto, T., Kawamoto, E., Takagi, Y., Akita, N., Hayashi, T., Park, E. J., Suzuki, K., & Shimaoka, M. (2017). Gap Junction-mediated regulation of endothelial cellular stiffness. *Scientific Reports*, *7*(1). https://doi.org/10.1038/s41598-017-06463-x

Palta, S., Saroa, R., & Palta, A. (2014). Overview of the coagulation system. *Indian Journal of Anaesthesia*, *58*(5), 515. https://doi.org/10.4103/0019-5049.144643

Parmar, K. M., Nambudiri, V., Dai, G., Larman, H. B., Gimbrone, M. A., & García-Cardeña, G. (2005). Statins exert endothelial Atheroprotective effects via the KLF2 transcription factor. *Journal of Biological Chemistry*, *280*(29), 26714-26719. https://doi.org/10.1074/jbc.c500144200

Parnell, E., Smith, B. O., Palmer, T. M., Terrin, A., Zaccolo, M., & Yarwood, S. J. (2012). Regulation of the inflammatory response of vascular endothelial cells by EPAC1. *British Journal of Pharmacology*, *166*(2), 434-446. https://doi.org/10.1111/j.1476-5381.2011.01808.x

Peghaire, C., Dufton, N. P., Lang, M., Salles-Crawley, I. I., Ahnström, J., Kalna, V., Raimondi, C., Pericleous, C., Inuabasi, L., Kiseleva, R., Muzykantov, V. R., Mason, J. C., Birdsey, G. M., & Randi, A. M. (2019). The transcription factor ERG regulates a low shear stress-induced anti-thrombotic pathway in the microvasculature. *Nature Communications*, *10*(1). https://doi.org/10.1038/s41467-019-12897-w

Pober, J. S., & Sessa, W. C. (2007). Evolving functions of endothelial cells in inflammation. *Nature Reviews Immunology*, *7*(10), 803-815. https://doi.org/10.1038/nri2171

Reglero-Real, N., Colom, B., Bodkin, J. V., & Nourshargh, S. (2016). Endothelial cell Junctional adhesion molecules. *Arteriosclerosis, Thrombosis, and Vascular Biology*, *36*(10), 2048-2057. https://doi.org/10.1161/atvbaha.116.307610

Ruan, G., & Kazlauskas, A. (2012). VEGF-A engages at least three tyrosine kinases to activate PI3K/Akt. *Cell Cycle*, *11*(11), 2047-2048. https://doi.org/10.4161/cc.20535

Sako, K., Fukuhara, S., Minami, T., Hamakubo, T., Song, H., Kodama, T., Fukamizu, A., Gutkind, J. S., Koh, G. Y., & Mochizuki, N. (2008). Angiopoietin-1 induces krüppel-like factor 2 expression through a Phosphoinositide 3-Kinase/AKT-dependent activation of Myocyte enhancer factor 2. *Journal of Biological Chemistry*, *284*(9), 5592-5601. https://doi.org/10.1074/jbc.m806928200

Schwartz, S. (2018). Faculty opinions recommendation of endothelial fluid shear stress sensing in vascular health and disease. *Faculty Opinions – Post-Publication Peer Review of the Biomedical Literature*. https://doi.org/10.3410/f.726183126.793553301

Shen, Q., Wu, M., & Yuan, S. (2009). Endothelial contractile cytoskeleton and microvascular permeability. *Cell Health and Cytoskeleton*, *Volume 1*, 43-50. https://doi.org/10.2147/chc.s5118

Soliman, S. (2019). *Brain Endothelial Nitric Oxide Mediates Increased Expression of Astrocyte-derived VEGF in the Pathogenesis of Cerebral Cavernous Malformations* [Master's thesis]. https://escholarship.org/uc/item/86r4q6sz

Stamatovic, S. M., Sladojevic, N., Keep, R. F., & Andjelkovic, A. V. (2015). PDCD10 (CCM3) regulates brain endothelial barrier integrity in cerebral cavernous malformation type 3: Role of CCM3-ERK1/2-cortactin cross-talk. *Acta Neuropathologica*, *130*(5), 731-750. https://doi.org/10.1007/s00401-015-1479-z

Sukriti, S., Tauseef, M., Yazbeck, P., & Mehta, D. (2014). Mechanisms regulating endothelial permeability. *Pulmonary Circulation*, *4*(4), 535-551. https://doi.org/10.1086/677356

Szmitko, P. E., Wang, C., Weisel, R. D., De Almeida, J. R., Anderson, T. J., & Verma, S. (2003). New markers of inflammation and endothelial cell activation. *Circulation*, *108*(16), 1917-1923. https://doi.org/10.1161/01.cir.0000089190.95415.9f

Taddei, A., Giampietro, C., Conti, A., Orsenigo, F., Breviario, F., Pirazzoli, V., Potente, M., Daly, C., Dimmeler, S., & Dejana, E. (2008). Endothelial adherens junctions control tight junctions by VE-cadherin-mediated upregulation of claudin-5. *Nature Cell Biology*, *10*(8), 923-934. https://doi.org/10.1038/ncb1752

THI, M. M., IACOBAS, D. A., IACOBAS, S., & SPRAY, D. C. (2007). Fluid shear stress Upregulates vascular endothelial growth factor gene expression in osteoblasts. *Annals of the New York Academy of Sciences*, *1117*(1), 73-81. https://doi.org/10.1196/annals.1402.020

Thomas, B., & Sumam, K. (2016). Blood flow in human arterial System-A review. *Procedia Technology*, *24*, 339-346. https://doi.org/10.1016/j.protcy.2016.05.045

Ting, L. H., Jahn, J. R., Jung, J. I., Shuman, B. R., Feghhi, S., Han, S. J., Rodriguez, M. L., & Sniadecki, N. J. (2012). Flow mechanotransduction regulates traction forces, intercellular forces, and adherens junctions. *American Journal of Physiology-Heart and Circulatory Physiology*, *302*(11), H2220-H2229. https://doi.org/10.1152/ajpheart.00975.2011

Tsuji, S., Washimi, K., Kageyama, T., Yamashita, M., Yoshihara, M., Matsuura, R., Yokose, T., Kameda, Y., Hayashi, H., Morohoshi, T., Tsuura, Y., Yusa, T., Sato, T., Togayachi, A., Narimatsu, H., Nagasaki, T., Nakamoto, K., Moriwaki, Y., Misawa, H., … Imai, K. (2017). HEG1 is a novel mucin-like membrane protein that serves as a diagnostic and therapeutic target for malignant mesothelioma. *Scientific Reports*, *7*(1). https://doi.org/10.1038/srep45768

Umezawa, Y., Akiyama, H., Okada, K., Ishida, S., Nogami, A., Oshikawa, G., Kurosu, T., & Miura, O. (2017). Molecular mechanisms for enhancement of stromal cell-derived factor 1–induced chemotaxis by platelet endothelial cell adhesion molecule 1 (PECAM-1). *Journal of Biological Chemistry*, *292*(48), 19639-19655. https://doi.org/10.1074/jbc.m117.779603

Versari, D., Daghini, E., Virdis, A., Ghiadoni, L., & Taddei, S. (2009). Endothelial dysfunction as a target for prevention of cardiovascular disease. *Diabetes Care*, *32*(suppl_2), S314-S321. https://doi.org/10.2337/dc09-s330

Wang, M., Hao, H., Leeper, N. J., & Zhu, L. (2018). Thrombotic regulation from the endothelial cell perspectives. *Arteriosclerosis, Thrombosis, and Vascular Biology*, *38*(6). https://doi.org/10.1161/atvbaha.118.310367

Whitehead, K. J., Adams, N. W., Marchuk, J. A., & Li, D. Y. (2004). Ccm1 is required for arterial morphogenesis: Implications for the etiology of human cavernous malformations. *Development*, *131*(6), 1437-1448. https://doi.org/10.1242/dev.01036

Yuan, S. Y., & Rigor, R. R. (2010). Introduction. In *Regulation of endothelial barrier function*. Morgan & Claypool Publishers.

Zhang, R., Li, X., & Boggon, T. J. (2015). Structural analysis of the KRIT1 ankyrin repeat and FERM domains reveals a conformationally stable ARD–FERM interface. *Journal of Structural Biology*, *192*(3), 449-456. https://doi.org/10.1016/j.jsb.2015.10.006

Zhou, Z., Tang, A. T., Wong, W., Bamezai, S., Goddard, L. M., Shenkar, R., Zhou, S., Yang, J., Wright, A. C., Foley, M., Arthur, J. S., Whitehead, K. J., Awad, I. A., Li, D. Y., Zheng, X., & Kahn, M. L. (2016). Cerebral cavernous malformations arise from

endothelial gain of MEKK3–KLF2/4 signalling. *Nature*, *532*(7597), 122-126. https://doi.org/10.1038/nature17178